






RESEARCH ARTICLE

The fungal *Clitocybe nebularis* lectin binds distinct cell surface glycoprotein receptors to induce cell death selectively in Jurkat cells

Milica Perišić Nanut¹  | Simon Žurga¹ | Špela Konjar¹  | Mateja Prunk¹  | Janko Kos²  | Jerica Sabotič¹ 

¹Department of Biotechnology, Jožef Stefan Institute, Ljubljana, Slovenia

²Faculty of Pharmacy, University of Ljubljana, Ljubljana, Slovenia

Correspondence

Jerica Sabotič, Department of Biotechnology, Jožef Stefan Institute, Jamova cesta 39, 1000 Ljubljana, Slovenia.

Email: jerica.sabotic@ijs.si

Funding information

This research was funded by the Research Agency of the Republic of Slovenia, grant number P4-0127 to J.K.

Abstract

Clitocybe nebularis lectin (CNL) is a GalNAc β 1-4GlcNAc-binding lectin that exhibits an antiproliferative effect exclusively on the Jurkat leukemic T cell line by provoking homotypic aggregation and dose-dependent cell death. Cell death of Jurkat cells exhibited typical features of early apoptosis, but lacked the activation of initiating and executing caspases. None of the features of CNL-induced cell death were effectively blocked with the pan-caspase inhibitor or different cysteine peptidase inhibitors. Furthermore, CNL binding induced Jurkat cells to release the endogenous damage-associated molecular pattern molecule high-mobility group box 1 (HMGB1). A plant lectin with similar glycan-binding specificity, *Wisteria floribunda* agglutinin (WFA) showed less selective toxicity and induced cell death in Jurkat, Tall-104, and Hut-87 cell lines. HMGB1 release was also detected when Jurkat cells were treated with WFA. We identified the CD45 and CD43 cell surface glycoproteins on Jurkat cells as the main targets for CNL binding. However, the blockade of CD45 phosphatase activity failed to block either CNL-induced homotypic agglutination or cell death. Overall, our results indicate that CNL triggers atypical cell death selectively on Jurkat cells, suggesting the potential applicability of CNL in novel strategies for treating and/or detecting acute T cell leukemia.

KEYWORDS

CD45, cytotoxicity, homotypic aggregation, lectin, T cell leukemia

Abbreviations: β 4GalNAcTs, β 4-N-acetylgalactosaminyltransferases; CNL, *Clitocybe nebularis* lectin; DAMP, danger-associated molecular patterns; FITC, fluorescein isothiocyanate; GAPDH, glyceraldehyde 3-phosphate dehydrogenase; HMGB1, high mobility group box 1; ICAM, intercellular adhesion molecule; LacdiNAc, GalNAc β 1-4GlcNAc or N,N'-diacetylglucosamine; PBMCs, peripheral blood mononuclear cells; PTP, protein tyrosine phosphatase; RIPK3, receptor-interacting serine/threonine-protein kinase 3; TMRM, tetramethylrhodamine methyl ester; PI, propidium iodide; SF3A1, splicing factor 3 subunit 1; WFA, *Wisteria floribunda* agglutinin.

This is an open access article under the terms of the Creative Commons Attribution-NonCommercial-NoDerivs License, which permits use and distribution in any medium, provided the original work is properly cited, the use is non-commercial and no modifications or adaptations are made.

© 2022 The Authors. *The FASEB Journal* published by Wiley Periodicals LLC on behalf of Federation of American Societies for Experimental Biology.

1 | INTRODUCTION

Cell surface glycans play important roles in numerous biological processes. Specific surface glycosylation patterns are distinctive for certain cell types^{1,2} but can also vary, depending on the environment and functional state of the cells.^{2,3} Changes in glycan expression actively direct a variety of biological processes.^{2,4,5} Neoplastic transformation is accompanied by profound alterations in both N- and O-glycosylation in healthy cells, leading to the overexpression of specific glycans.⁶ For example, the aberrant O-glycans expressed on cancer cell surfaces occur as saccharide components of membrane-bound N-acetylgalactosamine (O-GalNAc) glycoproteins (T and Tn antigen) and glycolipids (Lewis a and Lewis x). Mucin, a heavily O-GalNAc-glycosylated protein, is overexpressed and subsequently secreted by cancer cells, especially at the last stages of malignant progression. Certain glycosylation patterns are often specific to the type and stage of cancer and they are actively investigated as targets for immunotherapy and diagnostics.^{7,8}

Lectins are non-catalytic proteins that specifically bind distinct glycan structures. Lectins with known glycan-binding specificities are powerful tools for detecting changes in the carbohydrate structures of cellular glycoproteins and glycolipids.⁹ Furthermore, most lectins contain more than one carbohydrate-binding site and can cross-link cell surface carbohydrates.^{4,9} In this way, they participate in various cellular processes, including cell adhesion, migration, differentiation, apoptosis, and proliferation as well as intracellular trafficking, intercellular interactions, and recognition processes, especially in the immune system.⁵ However, the binding of a glycan target is only the initial step, and the associated downstream events must be scrutinized for a deeper understanding of the mechanism of lectin action that is still largely unknown.

In the past decade, in addition to antibodies, lectins of mostly plant origin have been used for diagnostic purposes, i.e., for identifying malignant or premalignant cells or as targeting vectors, due to their capacity to specifically recognize and distinguish subtle alterations in glycans on the cell surface.^{10,11} One such lectin is *Wisteria floribunda* agglutinin (WFA) which binds N-acetylgalactosaminides, particularly those with LacdiNAc. LacdiNAc is a unique N-glycan structure found in N- and O-glycans in vertebrates; however, it is rarely present in mammalian glycoproteins.^{12,13} In humans, the disaccharide group is only found on N-glycans and has been shown to play an important role in regulating the half-life of the circulating pituitary glyco-hormone lutropin in the blood.¹⁴ Interestingly, LacdiNAc levels on the non-reducing termini of N-glycans of cell surface glycoproteins are changed according to the

progression stages of human cancers, making LacdiNAc a potentially useful biomarker for cancer progression.^{15–17} Due to its high specificity, several recent studies have promoted the use of WFA for detecting overexpressed LacdiNAc or terminal GalNAc during cancer progression and growth.¹⁰ Not only did the abundance of LacdiNAc structures increase in certain cancers, but LacdiNAc was shown to regulate cancer behavior via modulating protein functions and signaling pathways in cells.¹⁸

We have previously isolated and biochemically characterized a lectin from the basidiomycete mushroom *Clitocybe nebularis*, designated *C. nebularis* lectin (CNL).^{12,19} CNL is a β -trefoil-type lectin that forms homodimers of 15.9 kDa subunits.¹⁹ This lectin specifically recognizes non-reducing N-acetylgalactosamine (GalNAc)-containing carbohydrates including N,N'-diacetyllactosediamine (GalNAc β 1-4GlcNAc, LacdiNAc) and human blood group A determinant GalNAc α 1-3(Fuc α 1-2) Gal β -containing carbohydrates.¹⁹ In this study, we used recombinant CNL,²⁰ which exhibits more restricted specificity for LacdiNAc than that of its natural counterpart, to obtain more specific and reproducible results. We explored the binding and mechanism of action of CNL on various human cell lines and found that it provoked homotypic aggregation and dose-dependent cell death selectively in Jurkat cells. Furthermore, we compared the effect of CNL to that of the plant lectin WFA with similar glycan-binding specificity and also identified the cell surface glycoproteins on Jurkat cells that are targets for CNL.

2 | MATERIALS AND METHODS

2.1 | Lectins

Recombinant fungal lectin CNL and the carbohydrate-binding mutants D20R-CNL (0-CNL) and N110D/L54R-CNL (Mono2R-CNL) were expressed in *Escherichia coli* and purified as described.²⁰ WFA was purchased from Vector laboratories (L-1350-5), and fluorescein isothiocyanate (FITC)-conjugated WFA was purchased from Hycultec (F-3101-2).

2.2 | Cell cultures

The following cell lines were used: non-differentiated histiocytic lymphoma cells (U937, American Type Culture Collection (ATCC), Manassas, VA, USA, CRL-1593.2), malignant non-Hodgkin lymphoma (NK-92, ATCC, CRL-2407), Burkitt's lymphoma (Raji, ATCC, CCL-86), acute T cell leukemia (Jurkat, ATCC, TIB-152), acute

lymphoblastic leukemia (Tall-104, ATCC, CRL-11386), hairy cell leukemia (Mo T, ATCC, CRL-8066), cutaneous T cell lymphoma (Hut-87, ATCC, TIB-161), acute promyelocytic leukemia (HL-60, ATCC, CCL-240), acute monocytic leukemia (THP-1, ATCC, TIB-202), myelogenous leukemia cells (K-562 ATCC, CCL-243), hepatocellular carcinoma cells (HepG2, ATCC, HB-8065), colorectal adenocarcinoma (CaCo-2, ATCC, HTB-37), neuroblastoma cells (SH-SY5Y, ATCC, CRL-2266), cervical cancer cells (HeLa, ATCC, CCL-2), glioblastoma astrocytoma (U251, formerly known as U-373 MG, ATCC, HTB-14), likely glioblastoma (U87MG, ATCC, HTB-14), prostatic carcinoma cell line (PC3, ATCC, CRL-1435), and Ras-transformed human breast epithelial cell line (MCF10A neo T derived from the MCF-10 cell line, ATCC, CRL-10317). The cells were grown under ATCC recommended culture conditions; heat-inactivated FBS and 1% penicillin/streptomycin were obtained from Gibco, USA. MCF10A neo T cells were grown in DMEM/F12 (1:1) medium supplemented with 5% (v/v) fetal bovine serum (HyClone), 1 µg/ml insulin, 0.5 µg/ml hydrocortisone, 50 ng/ml epidermal growth factor, 2 mM L-glutamine, 50 U/ml penicillin, and 50 µg/ml streptomycin (Sigma). Human Peripheral Blood Mononuclear Cells (PBMCs) healthy volunteers were provided by the Blood Transfusion Centre of Slovenia (Ljubljana, Slovenia). The cells were maintained at 37°C in a humidified atmosphere containing 95% air and 5% CO₂.

2.3 | Cell viability assay

The viability of different human cell lines following the addition of lectins was assessed using the MTS assay CellTiter 96 AQueous One Solution Cell Proliferation Assay (Promega, Madison, WI, USA) according to the manufacturer's instructions. The following human cell lines were used: U937, HL-60, NK-92, Jurkat, Tall-104, K-562, CaCo-2, SH-SY5Y, HeLa, PC3, U251, and MCF10A neo T. For the MTS cell viability assay, the number of seeded cells/well varied (0.7×10^4 – 6×10^4), depending on the cell type used. Cells were maintained in the appropriate culture media. Recombinant CNL (100 µg/ml) was added to the cells in 96-well plates, and cell viability was assessed after 48 h. For Jurkat cells, CNL in different concentrations (5–100 µg/ml) was added to the cells in 96-well plates, and cell viability was assessed after 48 h. When required, CA-074, CA-074Me, E64, and E64d inhibitors (5 µM, Bachem), lactose (0.1 M final concentration, Sigma), dasatinib (20 and 50 mM, Sigma), staurosporine (20 and 50 nM, Sigma), and NH₄Cl (10 mM) were added to the culture medium 1 h before the addition of lectin, and cell viability was assessed after the time points indicated.

Afterward, the assay was conducted according to the manufacturer's instructions, and absorbance was measured at 490 nm on the microplate reader Infinite M1000 (Tecan). The results are presented as percentages of the corresponding control cells.

2.4 | Cell death detection with flow cytometry

2.4.1 | Propidium iodide (PI) staining

The cytotoxicity of CNL was confirmed by flow cytometry analysis using PI (BD Bioscience). PI does not cross the cell membrane and only stains DNA in cells when the cell membrane is disintegrated. Cells were seeded in duplicate into a 24-well culture plate (6×10^5 cells/well for Tall-104 cells and 2×10^5 cells/well for other cell lines) and treated with CNL (50 µg/ml). When required, Z-VAD-FMK inhibitor (50 µM) was added to the culture medium 1 h before CNL treatment. After 4 h and 24 h of incubation, cells were washed with pre-warmed phosphate-buffered saline (PBS) and further stained with PI solution (30 µM) for 15 min at 37°C. Cells were then analyzed for cytotoxicity by flow cytometry with FACS Calibur (BD Bioscience, San Jose, CA, USA). The percentage of PI+cells was evaluated using FlowJo software (FlowJO, Ashland, OR, USA). The results are presented as relative fold increases of PI+compared to the corresponding control cells.

2.4.2 | Annexin V/PI staining

Apoptosis was detected and quantified using a FITC Annexin V Apoptosis Detection Kit I (BD Bioscience), in accordance with the manufacturer's instructions. Jurkat and Tall-104 cells were cultured in a 24-well plate (2×10^5 cells/well for Jurkat; 6×10^5 cells/well for Tall-104 cells) and treated with the recombinant lectins CNL, Mono2R-CNL, and 0-CNL (50 µg/ml) for 4 h and 24 h. Untreated cells were used as control. All experiments were performed in triplicate. When required, Kp7-6 antagonist (50 µM), lactose (0.1 M final concentration), or necrostatin-1 (30 µM/ml, Bachem) were added to the culture medium 1 h before the addition of lectin. After treatment, cells were washed with cold PBS and resuspended in 500 µl of binding buffer. FITC-labeled Annexin V (5 µl) and PI (5 µl) were added to the cells and incubated for 15 min in the dark. Cell apoptosis was analyzed using a FACS Calibur flow cytometer (BD Bioscience). The percentage of apoptotic cells (Annexin V+/PI–) was evaluated using FlowJo software, and the results were presented as the percentage of Annexin V+ (Annexin V+/PI–) and necrotic PI+

(Annexin V−/PI+ and Annexin V+/PI+) cells. The total number of events for each experiment was 20,000.

2.4.3 | YO-PRO-1 and PI staining

YO-PRO-1 (YP1) is a nuclear marker that binds to the DNA of dying cells⁶⁵ because its relatively large size (630 Da) prevents it from penetrating the intact plasma membrane of living cells. Apoptotic processes jeopardize membrane integrity and thus allow YP1 to enter cells. YP1 is a very sensitive marker of early cellular events reflecting an early and widespread plasma membrane injury that allows YP1 penetration into the cells. Apoptotic cells become permeant to YP1 but remain impermeant to PI, a dead cell stain. Different cell lines (Jurkat, MoT, THP-1, U87, Tall-104, NK-92, and U937) and human peripheral blood monocytes were seeded into a 24-well culture plate (2×10^5 cells/well) and treated with CNL (50 $\mu\text{g}/\text{ml}$) for 4 h and 24 h. Cells were then washed with PBS and stained with YP1 (YO-PRO-1 Iodide, Thermo Fisher Scientific) according to the manufacturer's instructions and analyzed with a FACS Calibur flow cytometer. Where indicated, the cells were treated with protein tyrosine phosphatase (PTP) CD45 inhibitor (50 μM , Sigma) 1 h before the addition of CNL.

2.4.4 | Determination of the reduction of mitochondrial membrane potential ($\Delta\psi\text{m}$)

The reduction of mitochondrial membrane potential ($\Delta\psi\text{m}$) was determined by staining cells with tetramethylrhodamine, methyl ester (TMRM) (Thermo Fisher Scientific), a cell-permeant dye that accumulates in active mitochondria with intact membrane potentials. Jurkat cells were seeded into a 24-well culture plate (2×10^5 cells/well) and treated with CNL (50 $\mu\text{g}/\text{ml}$) for 4 h and 24 h. Cells were then washed with PBS and stained with TMRM according to the manufacturer's instructions and analyzed with a FACS Calibur flow cytometer. The intensity of red fluorescence of the cells serves as a measure of $\Delta\psi\text{m}$. Data were analyzed with FlowJo software, and the results are presented as a percentage of $\Delta\psi\text{m}$ relative to the control (set to 100% $\Delta\psi\text{m}$).

2.5 | Apoptosis analysis using ImageStreamX

For apoptosis analysis, 1×10^6 Jurkat or TALL-104 cells were seeded into 12-well plates and incubated with CNL or WFA at 50 $\mu\text{g}/\text{ml}$ for 4 h and 24 h. After incubation, the

cells were washed with PBS and the nuclei were labeled with 5 $\mu\text{g}/\text{ml}$ Hoechst 33342 (Thermo Fisher Scientific) in PBS for 5 min. The cells were then washed once in PBS and resuspended at a cell density of $1\text{--}2 \times 10^7$ cells/ml in PBS containing 0.1 M lactose. Cell images of 20,000 cells were acquired with the ImageStreamX MKII imaging flow cytometer (AMNIS), and apoptosis analysis was performed using the apoptosis wizard in the IDEAS software (AMNIS).

2.6 | Measurement of Reactive Oxygen Species (ROS) production in Jurkat cells

Jurkat cells were cultured in a 24-well plate (2×10^5 cells/well) and pretreated with 0.5 mM N-acetyl-L-cysteine (NAC, Sigma) and 5 mM Ferostatin-1 (Sigma) for 4 h and 16 h before the addition of lectins. After pretreatment, cells were washed with Dulbecco's phosphate-buffered saline (DPBS, Invitrogen) and stained with 1 μM 5-(and-6-)-chloromethyl-2',7'-dichlorohydrofluorescein diacetate (CM-H2DCFDA, Invitrogen) for 30 min in Hanks' balanced salt solution (HBSS, Invitrogen) at 37°C. The cells were then incubated for 4 h in phenol red-free RPMI-1640 medium containing 10% FBS (recovery period), in the presence or absence of CNL (50 $\mu\text{g}/\text{ml}$), WFA (50 $\mu\text{g}/\text{ml}$) or 500 μM H_2O_2 (Life Technologies). Cells were centrifuged once and resuspended in HBSS. At least 2×10^4 cells per sample were analyzed by flow cytometry. The data were collected from triplicates Jurkat cell cultures. Untreated cells were used as control.

2.7 | Measurement of intracellular pH changes

Intracellular pH was measured using pHrodo[®] Green AM Intracellular pH Indicator (Thermo Fisher Scientific Inc.) in accordance with the manufacturer's guidelines. This reagent can quantify cellular cytosolic pH in the range of pH 9 to pH 4. Jurkat cells were cultured in a 24-well plate (2×10^5 cells/well) and pre-treated with 0.5 mM N-acetyl-L-cysteine (NAC, Sigma) and 0.5 mM N-Acetyl-L-alanine (NAA, Sigma) for 1 h and 16 h before the addition of lectins. After pre-treatment, cells were washed with Dulbecco's phosphate-buffered saline (DPBS, Invitrogen), then 10 μl pHrodo[™] Green AM was mixed with 100 μl of PowerLoad[™] concentrate and added to the cells in HBSS for 30 min at 37°C in accordance with the manufacturer's guidelines. Subsequently, the cells were plated to a 96-well plate (4×10^4 cells/well) and treated with CNL (50 $\mu\text{g}/\text{ml}$), WFA (50 $\mu\text{g}/\text{ml}$) for 4 h. Fluorescence was measured using the fluorescence microplate reader Infinite M1000

(Tecan) at an excitation wavelength of 509 nm and an emission wavelength of 533 nm. The data were collected from triplicates. Untreated cells were used as control.

2.8 | Measurement of intracellular calcium level

To measure the intracellular calcium level, we used Fluo-4 Calcium Imaging Kit. This reagent becomes fluorescent only after its entry into the cell. Jurkat cells (10^6 cells/well) in 0.5-ml HBSS were pre-loaded with Fluo-4 (1 μ M) diluted in PowerLoad™ Concentrate and incubated at 37°C for 30 min. The cells were washed with HBSS, resuspended in phenol red-free RPMI-1640 medium containing 10% FBS and treated with CNL (50 μ g/ml), WFA (50 μ g/ml) or phorbol-12-myristate-13-acetate (PMA) (10 ng/ml)/ionomycin (calcium ionophore) (500 ng/ml). After 1 min or 1 h incubation, the cells were analyzed using a FACS Calibur flow cytometer (BD Bioscience). At least 2×10^4 cells per sample were analyzed by flow cytometry. The data were collected from triplicates of Jurkat cell cultures. Untreated cells were used as control.

2.9 | Caspase activity assay

The activities of caspase-1, -3/7, and -6/8 were measured in total cell lysates of Jurkat cells (1×10^6 cells/ml) treated with CNL (20 μ g/ml) or staurosporine (1 μ M) for 4 h and 24 using the appropriate fluorescent substrates (from Bachem): YVAD-AFC, Ac-DEVD-AFC, and Ac-IETD-AFC for caspase-1, -3/7, and -6/8, respectively. Fluorescence was monitored continuously for 30 min using the fluorescence microplate reader Infinite M1000 (Tecan) at an excitation wavelength of 405 nm and emission wavelength of 535 nm. Results are presented as changes in fluorescence as functions of time.

2.10 | Western blot analysis of proteins

For the detection of proteins in cell lysates, cells were seeded into 12-well culture plates (1×10^6 cells/well). After treatment with or without 50 μ g/ml CNL, cells (Jurkat, U937, K562, Mo T, Tall-104, and NK-92) were washed with ice-cold PBS and lysed in cell lysis buffer (50 mM Tris/HCl, pH=8.0, 150 mM NaCl, 1% Triton X-100, 0.5% sodium deoxycholate, 0.1% SDS, 1 mM EDTA) supplemented with a cocktail of proteases and phosphatases for 30 min on ice. Lysates were centrifuged at 14,000 g at 4°C for 15 min. Protein concentrations were determined with the DC Protein Assay (Bio-Rad). Equal aliquots of

the protein were resolved by SDS/PAGE (12% gels). For high-mobility group box 1 (HMGB1) analysis, Jurkat and Tall-104 cells were cultured in a 24-well plate (6×10^5 cells/well) in FreeStyle 293 Expression Medium (Thermo Fisher Scientific) and treated with CNL and WFA (50 μ g/ml) for the time points indicated. Heat-induced (56°C for 5 min and ice for 10 min) and H₂O₂-induced (0.5 M for 24 h) necrosis served as a positive control, and treatment with staurosporine (1 μ M for 4 h) served as a negative control. Proteins from 100 ml of cell culture media were precipitated using the methanol/chloroform protocol⁶⁶ and subsequently resolved using SDS/PAGE. The proteins were transferred to the nitrocellulose membrane. Subsequently, membranes were incubated with 5% non-fat dried milk powder in PBS at room temperature for 1 h to block non-specific binding. Designated proteins were detected by incubating the membranes overnight at 4°C with primary antibodies in PBS with 5% non-fat dried milk powder. The following antibodies were used: polyclonal rabbit anti-CNL (BioGenes), monoclonal mouse anti-human CD45 (MAB1430, R&D system), and mouse monoclonal anti-human HMGB1 (MAB1690, R&D system). The membranes were washed four times for 10 min in PBS with 1% Tween and then incubated for 1 h with HRP-conjugated secondary antibodies (Jackson Immuno Research, West Grove, PA, USA). Finally, the membrane was washed four times for 5 min with PBS with 1% Tween. Membranes were re-probed with the primary antibodies anti-GABDH (Protein tech, 60004-1-1G) and secondary antibodies conjugated with the fluorescent dyes DyLight 650 or DyLight 550 (Thermo Fischer Scientific). The immunoreactive bands were visualized using chemiluminescence detection using Clarity Western ECL Substrate and ChemiDoc Imaging System (Bio-Rad).

2.11 | Immunofluorescence staining

Immunofluorescence staining was used to assess CNL localization in cells. For colocalization analyses, Jurkat and Tall-104 cells were treated with FITC-conjugated CNL or WFA (both at 100 μ g/ml) for 30 min and 180 min. After incubation, the cells were washed in PBS and cytocentrifuged (Stat Spin Cytofuge, Iris) onto glass slides. Cells were fixed with 4% paraformaldehyde in PBS for 15 min at room temperature, washed three times in PBS, and permeabilized with 0.1% Triton-X in PBS for 10 min at room temperature. The slides were then blocked with 3% bovine serum albumin in PBS for 1 h and incubated with primary antibodies for 1 h. The following primary antibodies were used: affinity-purified polyclonal rabbit anti-CNL (BioGenes), mouse monoclonal anti-human CD45, and CD43 (R&D systems).

Slides were washed three times in PBS and incubated for 1 h with the following Alexa-labeled secondary antibodies: goat anti-rabbit Alexa Fluor 488 (CST) and donkey anti-goat Alexa Fluor 647 (Invitrogen). Nuclei were stained with Hoechst 33342 (Thermo Fisher Scientific), and slides were mounted with Prolong Gold mounting media (Thermo Fisher Scientific).

Membranes were labeled with a membrane-embedded palmitoylated green fluorescent protein, coded by the pCAG-GFP plasmid (Addgene, MA, USA). Transfection of cells was performed one day in advance with Lipofectamine 2000 Reagent (Life Technologies), following the manufacturer's instructions.

The inhibition of lectin binding and/or its internalization was achieved by pre-incubation of CNL (10 µg/ml) for 30 min at 37°C in a growth medium containing lactose (0.1 M final concentration). All inhibitors were added to the cells 1 h prior to CNL treatment.

Immunostained cells were visualized with an LSM-710 confocal microscope (Carl Zeiss, Germany) equipped with UV (405 nm), Argon (488 nm and 514 nm), and HeNe (543 nm and 633 nm) lasers and under 63× magnification. The images were acquired and processed using ZEN software (Carl Zeiss).

2.12 | Membrane protein isolation, co-immunoprecipitation, and mass spectrometry

Jurkat cells were grown in appropriate media and harvested. Cells were centrifuged and washed two times in cold PBS. Cells were resuspended in fractionation buffer (250 mM sucrose, 20 mM HEPES, 10 mM KCl, 1.5 mM MgCl₂, 1 mM EDTA (Serva), 1 mM EGTA (Fluka), 1 mM dithiothreitol (DTT), pH 7.4) with protease inhibitor cocktail cOmplete™ ULTRA Tablets, Mini, EDTA-free (Roche). All subsequent steps were performed at 4°C. Cells were passed through a 27-gauge needle 10 times and then lysed in a Dounce homogenizer with 5 pestle strokes. The cell lysate was incubated for 20 min before centrifugation (5 min, 720 × g). The pellet was washed with fresh fractionation buffer, passed through the 27-gauge needle 10 times, and centrifuged again (10 min, 720 × g). The two supernatants were combined and centrifuged (20 min, 12,000 × g). The resulting supernatant was subjected to centrifugation in a Centrikon T-2070 ultracentrifuge (Kontron Instruments, Germany) in a TST 28.38 rotor for 45 min at 100,000 × g. The pellet was resuspended, passed through a 27-gauge needle 10 times, and centrifuged again (45 min, 100,000 × g). The pellet was dissolved in lysis buffer (50 mM HEPES, 250 mM NaCl, 0.1% (v/v) NP-40 (Igepal CA-630, Sigma), pH 7.0).

Membrane protein samples (50 µl) were then incubated with CNL (2 µg) in lysis buffer with or without lactose (0.05 M). CNL-target complexes were co-immunoprecipitated with the magnetic nanoparticles Dynabeads Protein G (Invitrogen) according to the manufacturer's instructions. Empty nanoparticles (25 µl) were labeled with 6 µg of affinity-purified rabbit anti-CNL (Biogenes) for isolation of CNL complexes. Labeled nanoparticles were added to mixtures of membrane protein samples pre-incubated with lectin and incubated for 30 min on a tube rotator. Nanoparticles were heated for 10 min at 95°C in SDS sample buffer with 20 mM DTT, and the proteins were resolved on precast 8% Precise™ Tris-Glycine gels (Thermo Fischer Scientific). Gels were silver-stained, individual bands were excised, following in-gel trypsin digestion, and identified by mass spectroscopy fingerprinting using an Orbitrap linear trap quadrupole Velos mass spectrometer coupled to a Proxeon nano-LC HPLC unit (Thermo Fisher Scientific). Results were analyzed using Scaffold MS software (Proteome Software).

2.13 | Aggregation

Jurkat, Tall-104 or HL-60 cells (2×10^4 cells in 150 µl complete media) were seeded into flat-bottom 96-well plates. Recombinant CNL, CNL mono, CNL-0, or WFA were added at 50 µg/ml, and lactose was added at 0.1 M. When required, dasatinib inhibitor (50 µM) or tunicamycin (1 µM, Sigma) were added to the culture medium 1 h (dasatinib) or 24 h (tunicamycin) before the addition of lectin. Transmission images of Jurkat and Tall-104 cells were acquired with the Axio observer (Carl Zeiss) under 10× magnification.

2.14 | Expression analysis of β4GalNAcT3 and β4GalNAcT4 with real-time quantitative PCR (qPCR)

Total RNA was extracted from the selected cell lines using TRIzol reagent (Life Technologies, USA) according to the manufacturer's instructions and quantified using a NanoDrop Spectrophotometer (Thermo Fisher Scientific). First-strand cDNA was synthesized from 1 µg of RNA using the High-Capacity cDNA Reverse Transcription Kit with RNase Inhibitor (Thermo Fisher Scientific) and random primers, according to the manufacturer's instructions. qPCR reactions were carried out for β4GalNAcT3 and β4GalNAcT4 coding genes and two reference genes (GAPDH and SF3A1, PrimerDesign, Southampton, UK) in each sample using FastStart Universal SYBR Green Master (Rox) (Roche Applied Science, Germany).

chemistry on a StepOnePlus Real-Time PCR System (Applied Biosystems, USA). All reactions were performed in a total volume of 10 μ l and contained 10-ng RNA equivalent cDNA and 200 nM of the coding gene set of sense and antisense primers or 250 nM of the reference gene primer mix. Previously published primers for β 4GalNAcT3 (5'-CTACAGCGCATTGTGAACGT-3' with 5'-TGGTTCTTCACAGGCACGAC-3')⁶⁷ and β 4GalNAcT4 (5'-CTGGCGTTTTTAACAGTGGC-3' with 5'-ATCCTC GTTGAGCTGGAGTT -3')⁶⁸ were used. Thermal cycles were set at 95°C for 10 min, followed by 45 cycles of 95°C for 10 s, 62°C for 20 s, and 72°C for 20 s, followed by the melt curve analysis. No template control reactions were included in the assays. PCR efficiencies were at least 80% for all primer pairs, and a single melting peak was observed for each primer pair. Relative gene expression was calculated upon normalization to two reference genes and corrected for primer-specific PCR efficiency as described previously.⁶⁹

2.15 | Statistical analyses

The results shown are representative of at least two independent experiments, each performed at least in duplicate, and are presented as means \pm SD. The student's *t*-test was used for statistical evaluation when two sets of values were compared. For comparison of three sets of values, one-way analysis of variance (ANOVA) was used, followed by Tukey's HSD test for post hoc comparisons; *p* < .05 was considered statistically significant.

3 | RESULTS

3.1 | CNL selectively kills Jurkat cells

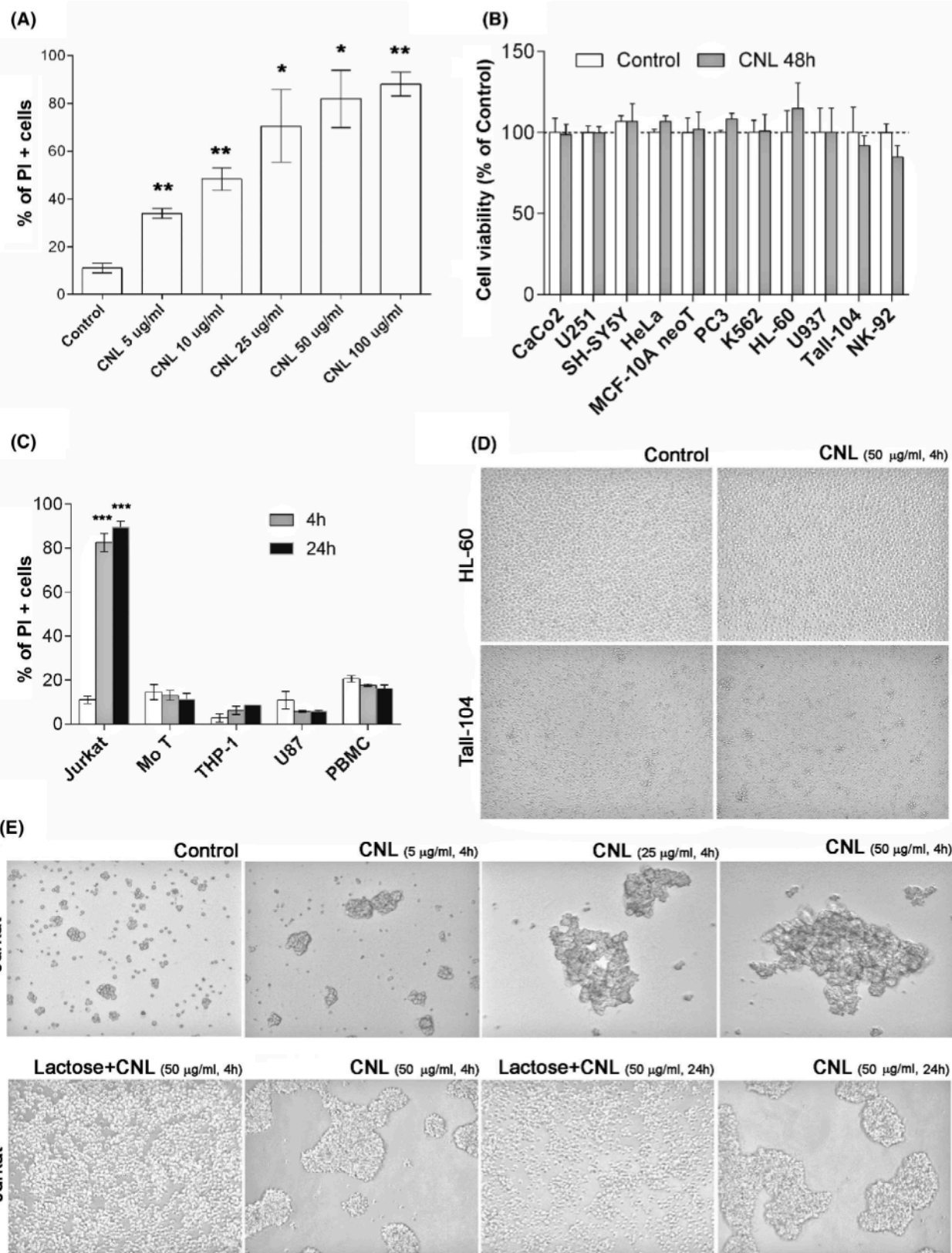
CNL treatment for 4 h significantly reduced Jurkat cell viability in a concentration-dependent manner (Figure 1A). In accordance with our previous results,²⁰ the number of viable Jurkat cells was significantly reduced after incubation with CNL at concentrations as low as 5 μ g/ml, and 100 μ g/ml CNL decreased the number of detected live cells by >80% (Figure 1A). To identify other cell lines susceptible to CNL cytotoxicity, we incubated several different myeloid (HL-60, U937, K562), lymphoid (Tall-104, NK-92, Hut-87), and several cancer cell lines of non-immune origin (CaCo₂, U251, SH-SY5Y, HeLa, MCF-10A neoT, PC3) with the highest used concentration of CNL (100 μ g/ml) for 48 h. However, no significant changes in their viability were detected (Figures 1B and S5). Moreover, PI staining and subsequent flow cytometry analysis of T cell leukemia cell lines (Mo T, Tall-104), an acute monocytic leukemia

cell line (THP-1), myeloid leukemia cell lines (K562, U937), lymphoma cell line (NK-92), a glioblastoma cell line (U87), and PBMCs showed no cytotoxicity after 4 h and 24 h of treatment with 100 μ g/ml CNL (Figures 1C and S1). Furthermore, no effect on the homotypic aggregation of myeloid (HL-60) and lymphoid (Tall-104, Hut-87) cells was detected after 4 h of treatment with 50 μ g/ml CNL (Figures 1D and S5). In contrast, 4 h incubations with different CNL concentrations showed a dose-dependent homotypic aggregation of Jurkat cells (Figure 1E). However, pretreatment with 0.1 M lactose, which binds to and blocks the carbohydrate-binding sites of CNL, abolished the agglutinating effect of CNL (Figure 1E).

3.2 | CNL induces apoptosis-like cell death without activation of major caspases

To examine the mode of cell death that CNL induces in Jurkat cells, we initially analyzed the changes in the cell mitochondrial membrane potential (ψ m) using TMRM. Flow cytometry analysis of TMRM staining of the cells incubated with CNL (50 μ g/ml) for 4 h and 24 h revealed a significant increase in the percentage of TMRM-negative cells only within the Jurkat cells. The percentage of TMRM-negative Jurkat cells did not significantly increase with prolonged CNL incubations (Figure 2A).

CNL-treated cells displayed reductions in cell size, as measured by forward scattering as well as increased binding of Annexin V (Figures 2B and S2). Together with simultaneous PI staining, this sensitive method detects early events that occur during apoptosis and distinguishes between apoptotic cells displaying externalization of phospholipid phosphatidylserine on the cell surface (Annexin V+) and dead cells that have already progressed to a loss of plasma membrane integrity (PI+).²¹ Incubation with 50 μ g/ml of CNL for 4 h resulted in approximately ~30% of apoptotic (Annexin V+/PI-) and ~40% of (primary or secondary) necrotic Jurkat cells (PI+). After 24 h of incubation, the percentage of Annexin V+ apoptotic cells decreased to <20%, and the percentage of necrotic cells (PI+) increased (Figures 2B and S2). Overall cell death increased after prolonged incubation with CNL, indicating also a time dependency of its cytotoxic effects. The increase in the ratio of Annexin V+ to PI+ cells suggests that primary apoptotic cells transitioned to late apoptotic (secondary necrotic) cells, implying apoptosis as a mode of cell death induced by CNL. Furthermore, pretreatment with 0.1 M lactose abolished the cytotoxic effects of CNL. As previously published,²⁰ both the non-glycan-binding mutant 0-CNL (CNL0) and the non-dimerizing CNL mutant Mono2R-CNL (CNL mono) showed no toxicity to Jurkat cells, even at 50 μ g/ml (Figure 2B).



CNL binding induced a typical apoptotic morphology of the cell nuclei. Using Hoechst 33342 membrane-permeable dye and imaging flow cytometer AMNIS, we performed

apoptosis analysis and showed clearly condensed DNA after 4 h and 24 h treatment with CNL, typical for cell apoptosis but not for cell necrosis (Figure 2C).

FIGURE 1 The effects of *Clitocybe nebularis* lectin (CNL) on different human cell lines. (A) The effects of 4 h of incubation with different CNL concentrations on Jurkat cells. Asterisks above bars indicate statistically significant differences ($*p < .05$; $**p < .01$) between the viability of control and CNL-treated cells. (B) The viability of different cell lines after 48 h of incubation with 100 $\mu\text{g}/\text{ml}$ of CNL (grey bars). Bars represent means \pm SD of the percentage of control cells (white bars), each assessed in three independent experiments. (C) The effects of 4 h (grey bars) and 24 h (black bars) of incubation with 100 $\mu\text{g}/\text{ml}$ of CNL on different human cell lines. The data were analyzed using one-way analysis of variance (ANOVA) where $*** (p < .001)$ indicates a significant difference in comparison with the untreated (white bars) control group. (D) Brightfield images of HL-60 and Tall-104 cells incubated with 50 $\mu\text{g}/\text{ml}$ of CNL for 4 h. (E) Brightfield images of homotypic aggregation of Jurkat cells after 4 h of incubation with different concentrations of CNL (upper panel). Pre-incubation with 0.1 M lactose (for 1 h) completely abrogated the homotypic aggregation of Jurkat cells after 4 h and 24 h of incubation with 50 $\mu\text{g}/\text{ml}$ of CNL (lower panel). Images were acquired at 10 \times magnification

The extrinsic pathway of apoptosis is triggered by the binding of ligands to their cognate death receptors, such as Fas/FasL. Therefore, the ability of CNL to induce cell death by association with death receptors was investigated. Jurkat cells were pretreated with Fas/FasL antagonist Kp7-6 (0.5 mM) for 1 h and then treated with CNL (50 $\mu\text{g}/\text{ml}$) for an additional 4 h and 24 h. The Fas/FasL antagonist had no significant impact on the percentage of apoptotic (Annexin V+) or necrotic (PI+) Jurkat cells at both time points examined (Figure 2D).

Caspases are vital mediators of apoptosis. To examine the activation of the caspase cascade, we first pretreated cells with Z-VAD-FMK (50 μM), a broad-spectrum irreversible inhibitor of the caspase family, and incubated the cells with CNL (50 $\mu\text{g}/\text{ml}$) for an additional 4 h and 24 h (Figure 2D). Pretreatment with Z-VAD-FMK did not significantly alter the cytotoxicity of CNL at both time points examined, indicating that caspases do not participate in the execution of cell death initiated by CNL binding (Figure 2D). To confirm this assumption, the enzymatic activity of the main activator (caspase-8) and effector (caspases-3/7) caspases was measured 2 h and 4 h after the addition of CNL (50 $\mu\text{g}/\text{ml}$). Staurosporine (1 μM)-treated Jurkat cells served as positive controls. At both time points, caspase-3/7 and caspase-8/6 activities did not increase in CNL-treated Jurkat cells, whereas their activities were significantly increased upon staurosporine treatment (Figure 2E).

3.3 | CNL induces programmed necrosis-like cell death

Recent studies indicate that some forms of necrotic cell death are regulated and controlled by inducer-specific cellular factors and susceptible to distinct inhibitors. However, contrary to a multistep cascade driving apoptotic cell death, only single, inducer-specific events have been associated with some types of programmed necrosis. For the best-studied form of necrotic cell death, pyroptosis, caspase-1 activation has been shown to be the key inducer. Caspase-1, a member of the family of inflammatory

caspases, is also known as the IL-1 β -converting enzyme. However, no caspase-1 activation occurred 2 h or 4 h after CNL treatment (Figure 2F). Lysosomal proteolytic enzymes, particularly lysosomal cathepsins, were shown to be involved in another form of programmed necrosis, termed lysosome-mediated necrosis. To determine the role of lysosomal proteases in CNL-induced cell death, we used cathepsin inhibitors and the lysosomotropic agent NH_4Cl . Jurkat cells were pre-incubated for 1 h with each of the irreversible protease inhibitors, and the cells were incubated for an additional 4 h or 24 h with CNL (Figure 2G). Our results showed no significant decrease in CNL cell toxicity in Jurkat cells pre-incubated with broad-spectrum cysteine protease inhibitor E64 (5 μM) or its cell-permeant form E64d (5 μM). Furthermore, pre-incubation with CA-074 (5 μM), a known cathepsin B inhibitor, and its methylated form CA-074-Me (5 μM), the only inhibitor known to block all forms of programmed necrotic cell death,^{22,23} did not significantly decrease the cytotoxic effect of CNL on Jurkat cells. The cathepsin L-specific inhibitor II (10 nM) also exerted no effects on Jurkat cell viability upon the addition of CNL. Finally, we found that the lysosomotropic agent NH_4Cl (500 μM) did not affect CNL cytotoxicity at either of the time points analyzed (Figure 2G). Taken together, our findings suggest that lysosomal (pH-dependent) proteases are not critically involved in the CNL-induced cell death pathway.

Finally, while apoptotic cells retain their intracellular content, a form of necrotic cell death termed necroptosis is characterized by the release of intracellular danger-associated molecular patterns (DAMP) such as HMGB1. This form of necrotic cell death is induced by specific death receptors, such as TNF- α , TRAIL, or poly-I:C, in the absence of caspase activation. HMGB1 is one of the most extensively studied DAMPs and is involved in the pathogenesis of many inflammatory diseases. HMGB1 may be passively released into the extracellular space as a prototypical DAMP from dying cells or actively secreted by stressed or activated cells present in any tissue.²⁴ Western blot analysis showed that HMGB1 was released into the cell culture medium as early as 2 h after the addition of CNL, increasing further with incubation

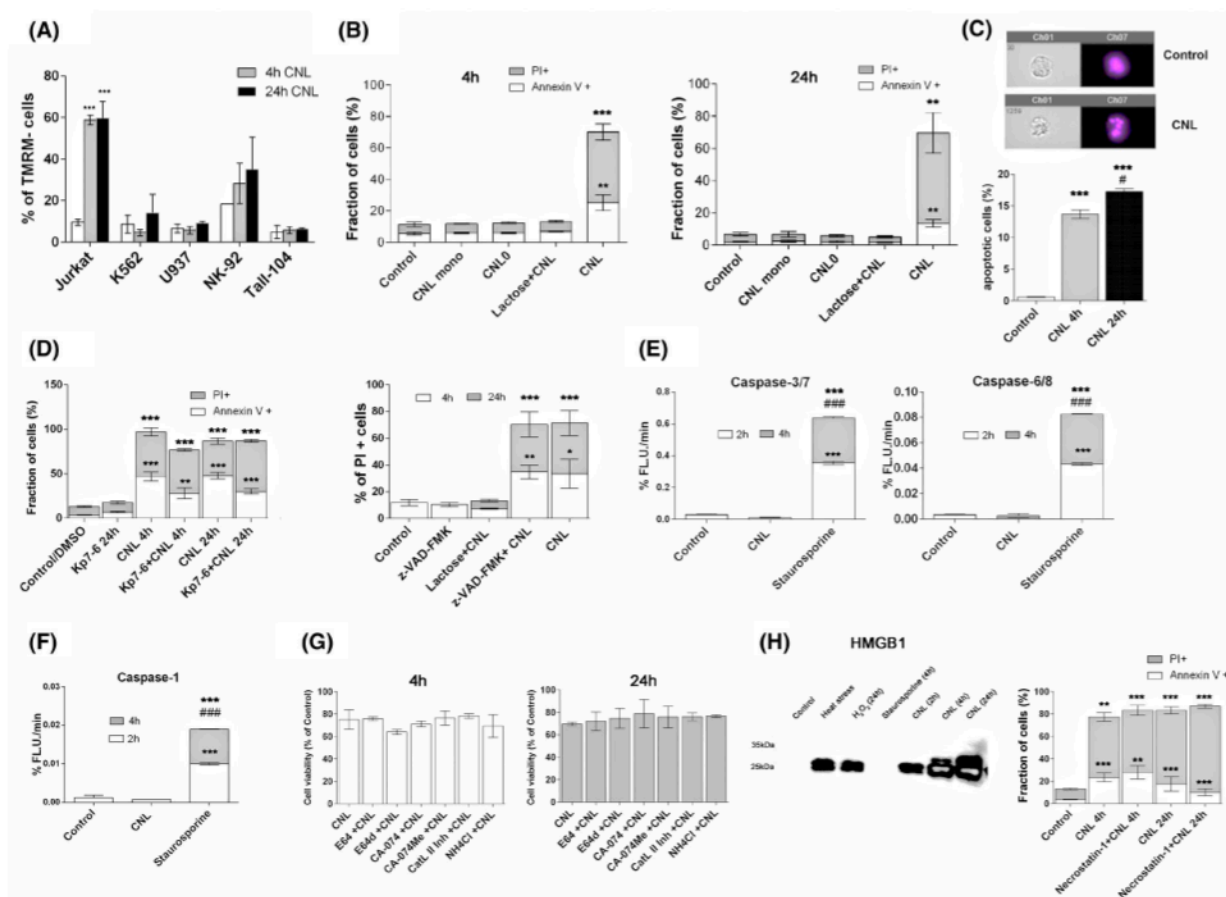


FIGURE 2 *Clitocybe nebularis* lectin (CNL) kills Jurkat cells through apoptosis-like and necrosis-like cell death. (A) Mitochondrial membrane (TMRM) staining of different cell lines incubated for 4 h (grey bars) and 24 h (black bars) with 50 µg/ml of CNL. White bars represent untreated control cells. The data were analyzed using one-way analysis of variance (ANOVA) where ***($p < .001$) indicates significant difference in comparison with the untreated (control) group. (B) Annexin V/PI staining of Jurkat cells incubated with non-dimerizing CNL mutant Mono2R-CNL (CNL mono), non-glycan-binding mutant CNL0, and recombinant CNL. Stacked bars represent the percentage of Annexin V+ (white bars) and PI+ (grey bars). Jurkat cells after 4 h (left) and 24 h (right) of incubation with 50 µg/ml of CNL or its mutant forms. Asterisks above bars indicate statistically significant differences (** $p < .01$; *** $p < .001$) between the control and CNL-treated cells. (C) Apoptosis analysis of Jurkat cells using Hoechst 33342 after 4 h (grey bar) and 24 h (black bar) of incubation with CNL. Control cell staining is represented with the white bar. Inserts show Hoechst 33342 staining of representative control cell (top) and a cell treated with CNL for 4 h (bottom). The data were analyzed using one-way ANOVA where ***($p < .001$) indicates significant difference in comparison with the untreated (control) group; #($p < .05$) indicates significant difference in comparison with the 4 h treated group. (D) Annexin V/PI staining of Jurkat cells pre-incubated with Fas/FasL (left) antagonist for 1 h prior to incubation with CNL. Stacked bars represent the percentage of Annexin V+ (white bars) and PI+ (grey bars) cells after 4 h and 24 h of incubation with 50 µg/ml of CNL. PI staining of cells pre-incubated with caspase inhibitor Z-VAD-FMK (right) for 1 h prior to 4 h (white superimposed bars) or 24 h (grey superimposed bars) of incubation with 50 µg/ml of CNL. The data were analyzed using one-way analysis of variance (ANOVA) where *($p < .05$); **($p < .01$); ***($p < .001$) indicate significant difference in comparison with the untreated (control) group. (E) The activity of caspase-3/7 and caspase-6/8 in Jurkat cell lysates 2 h (white superimposed bars) and 4 h (grey superimposed bars) after the addition of CNL (50 µg/ml) or staurosporine (1 µM). The data were analyzed using one-way ANOVA where ***($p < .001$) indicates significant difference in comparison with the untreated (control) group; ###($p < .001$) indicates significant difference in comparison with the 2 h treated group. (F) The activity of caspase-1 in Jurkat cell lysates 2 h (white superimposed bars) and 4 h (grey superimposed bars) after the addition of 50 µg/ml of CNL or staurosporine (1 µM). The data were analyzed using one-way ANOVA where ***($p < .001$) indicates a significant difference in comparison with the untreated (control) group; ###($p < .001$) indicates a significant difference in comparison with the 2 h treated group. (G) Jurkat cells after 4 h and 24 h of incubation with 50 µg/ml of CNL. The viability of Jurkat cells after 1 h of pretreatment with different protease inhibitors and lysosomotropic agent NH₄Cl followed by 4 h (white bars) and 24 h (grey bars) of incubation with 50 µg/ml of CNL. (H) Western blot analysis of the release of high-mobility group box 1 (HMGB1) into the cell culture medium after the induction of necrosis (by H₂O₂ and heat stress), apoptosis (1 µM staurosporine), and the addition of CNL at indicated time points (left). Annexin V/PI staining of Jurkat cells pre-incubated with necrostatin-1 (30 µM/ml) for 1 h prior to incubation with CNL (right). Stacked bars represent the percentage of Annexin V+ (white bars) and PI+ (grey bars). Asterisks above bars indicate statistically significant differences (** $p < .01$; *** $p < .001$) between the control and CNL-treated cells

time. In the cell culture medium of control cells and cells incubated with staurosporine, which at 1 μ M induces apoptosis of Jurkat cells, HMGB1 remained below the detection level (Figure 2H). Receptor-interacting serine/threonine-protein kinase 3 (RIPK3) and mixed lineage kinase domain-like pseudokinase were identified as essential key players in this process, which is often associated with the initiation of an inflammatory immune response. However, when the necrostatin-1-specific inhibitor of RIPK3 was added before the addition of CNL, no significant differences were observed in the percentage of Annexin V+ or PI+ cells compared with CNL-treated cells (Figure 2H).

3.4 | CNL binds to the surface proteins of Jurkat cells but is not internalized

Confocal microscopy showed that CNL binds to the cell surface of Jurkat cells 5 min upon addition, and the overall pattern of its localization does not change even after 3 h of incubation (Figure S3). Experiments with the mutant forms of CNL showed that the bivalency of the dimer-forming CNL is required for binding to the cell surface (Figures 3A and S3). After 1 h, 0-CNL (non-binding mutant of CNL) or Mono2R-CNL (monovalent non-dimerizing mutant of CNL) did not bind to Jurkat cells. As in the previous experiments, the 30 min pre-incubation of CNL with the competitive inhibitor lactose (0.1 M) completely abolished CNL binding to the cell surface of Jurkat cells (Figure 3A). Despite permeabilization during staining with anti-rCNL antibodies, the immunocytochemical analysis showed CNL staining only on the cell surface of U937 and Jurkat cells (Figure S3). Further analysis of Jurkat and HeLa cells showed that CNL colocalizes with membrane-embedded palmitoylated GFP (Figure 3B). The co-localization of mutant forms of CNL, 0-CNL, and Mono2R-CNL in Jurkat and HeLa cells could not be detected due to low binding and consequent low fluorescence intensity.

Flow cytometry analysis showed that CNL binds to almost all Jurkat cells, whereas it binds to only a fraction of NK-92, Tall-104, and K562 cells. The binding of CNL to Mo T and U937 cells was negligible (Figure 3C). The percentage of Jurkat cells that bind CNL did not change even after 24 h, whereas the percentage of Tall-104 cells that bind CNL increased after 24 h.

Western blot analysis of cell lysates after 24 h of incubation with CNL showed several immunoreactive bands. In the Jurkat cell lysate, the most pronounced bands were approximately 130 kDa; these were also present, although much less pronounced, in the cell lysates of Mo T, Tall-104, and NK-92 cells (Figure S4).

3.5 | CNL binds to a restricted set of cell surface glycoproteins on Jurkat cells

Jurkat cell membrane proteins were isolated, incubated with CNL, and the complexes were isolated by co-immunoprecipitation to determine CNL target proteins. By mass spectrometry analysis and comparison of co-immunoprecipitation in the absence or presence of lactose, two membrane glycosylated proteins and three proteins with non-membrane localization were identified as targets of CNL (Table 1). The best peptide coverage was obtained for glycosylated protein tyrosine phosphatase receptor type C or CD45 antigen (25 and 21 unique peptides). Leukosialin (also known as sialophorin, gp115, or CD43) was the second membrane-bound glycosylated target (3 peptides). CD43 is a large sialoglycoprotein that is abundantly expressed by cells of hematopoietic origin, including both CD4+ and CD8+ T cells.²⁵ Low coverage was obtained for glycosylated lysosomal/secreted protease cathepsin D (4 peptides). Cytoplasmic heat shock protein HSP90-beta (3 peptides) and importin subunit beta-1 found in the nuclear envelope (4 peptides) are presumably contaminants from the membrane purification protocol.

In Jurkat and Tall-104 cells, CNL colocalized with both CD45 and CD43 (Figure 4A,B) after 30 min and 3 h. CNL exhibited stronger colocalization with CD45, and CNL staining was much more pronounced on Jurkat cells compared to Tall-104 and its localization did not change throughout the duration of the experiment.

The CD45 (leukocyte common) antigen is one of the most abundant cell surface glycoproteins, comprising up to 10% of the cell surface area, on all hematopoietic cells and their precursors, except for mature erythrocytes and platelets.²⁶ Immune system neoplasia, including rapidly proliferating lymphomas and leukemias, ubiquitously expresses CD45 and is dependent on its PTP activity.²⁷ Multiple CD45 isoforms can be generated by complex alternative splicing of exons in the extracellular domain. The expression of different CD45 isoforms is cell type-specific and dependent on the differentiation and activation state of the cells.²⁸ However, the expression patterns for a given population are not absolute, and a single cell type can express multiple CD45 isoforms.²⁹ Our western blot analysis showed that both NK-92 and Tall-104 cells exhibit higher CD45 expression than Jurkat cells (Figure 5A). CD45 expression was low in U937 cell lysates and below the detection level in K562 and glioblastoma U251 and U87 cell lysates. Analysis of the expression of different CD45 isoforms showed that Jurkat cells expressed different CD45 isoforms, with CD45RA as the predominant form. In Tall-104 cells, the CD45RO was the predominant form (Figure 5B). CD45 has an intrinsic tyrosine phosphatase activity and has been implicated

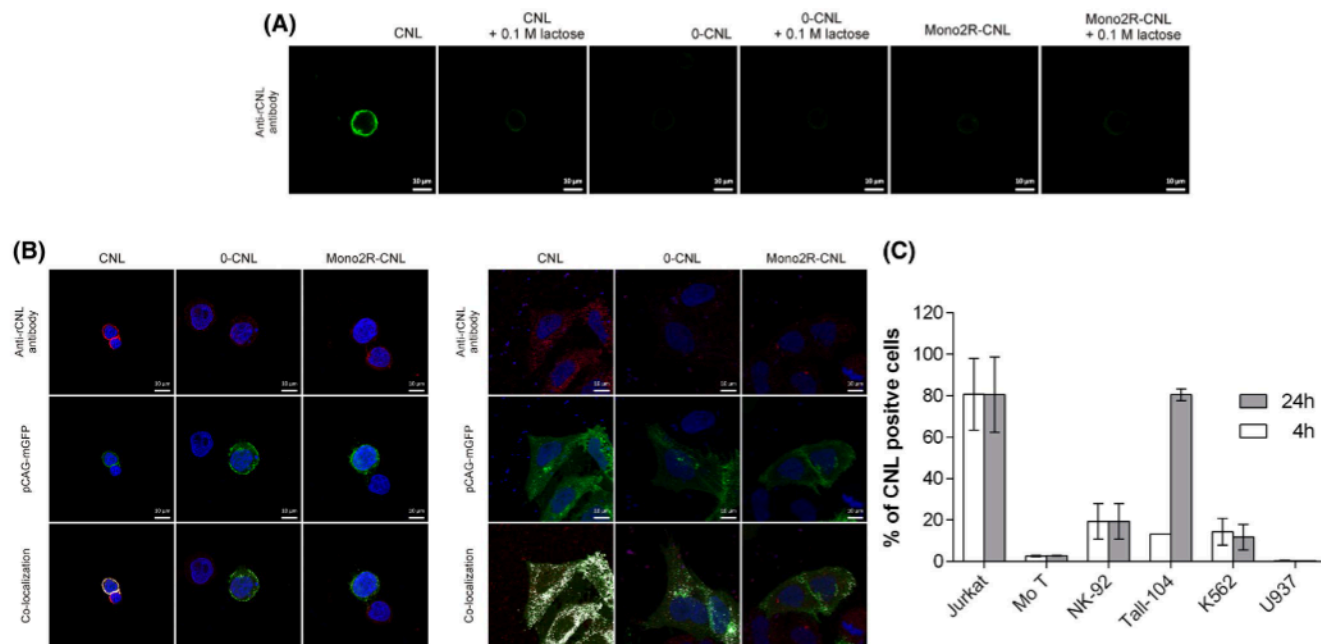


FIGURE 3 The intensity of *Clitocybe nebularis* lectin (CNL) binding to different cell lines and its localization upon binding. (A) The localization of CNL and the mutants 0-CNL and Mono2R-CNL in the absence or presence of 0.1 M lactose in Jurkat cells after 60 min of incubation. Cells were stained with rabbit polyclonal anti-rCNL antibodies and secondary goat anti-rabbit antibodies conjugated with Alexa Fluor 488. Images were acquired at 63× magnification. (B) The localization of CNL, 0-CNL, and Mono2R-CNL 3 h after the addition to Jurkat (left) and HeLa (right) cells transfected with the pCAG-mGFP plasmid for membrane labeling. For CNL labeling, cells were stained with rabbit anti-CNL antibodies and secondary goat anti-rabbit antibodies conjugated with Alexa Fluor 555. DAPI staining was used to label nuclei (blue). Images were taken at 63× magnification. Co-localization analysis was performed with ZEN software and the threshold values were determined using single-stained controls. Pixels with significant intensity levels of both labels are shown in white. (C) Flow cytometry analysis of CNL binding to different cell lines after 4 h (white bars) and 24 h (grey bars)

TABLE 1 Identification of *Clitocybe nebularis* lectin targets by peptide mass fingerprinting

Protein (UniProt)	Identified protein (gene)	Glycoprotein	Cellular localization	Number of unique peptides	
				SampleCNL 1	SampleCNL 2
Q92729	Protein tyrosine phosphatase receptor type C—CD45 (PTPRU)	N-glycosylated	Membrane	25	21
P16150	Leukosialin—CD43 (SPN)	O-glycosylated	Membrane	4	
P07339	Cathepsin D (CTSD)	N-glycosylated	Lysosome, Secreted	4	
Q14974	Importin subunit beta-1 (KPNB1)	No	Cytoplasm, Nucleus envelope	4	
P08238	Heat shock HSP 90-beta (HSP90AB1)	Predicted O-glycosylated	Cytoplasm	3	

in cell proliferation, signaling, and differentiation, and is associated with the B cell receptor during signaling.³⁰ As CD45 phosphatase activity modulates the threshold of T-cell receptor signaling and activates numerous inhibitory factors, it plays a critical role for T-cell proliferation and survival by regulating the Src family tyrosine kinases, such as lymphocyte-specific protein tyrosine kinase and the proto-oncogene protein tyrosine kinases

Fyn (p59-FYN) and Lyn. Therefore, we examined whether the inhibitor of CD45-associated PTP can abolish the cytotoxic effects of CNL on Jurkat cells. Flow cytometric analysis after staining with YO-PRO-1 (YP1), a nuclear marker that binds to the DNA of dying cells showed that the pre-treatment of cells with PTP CD45 inhibitor did not significantly alter the percentage of YO-PRO-1 +, dying Jurkat cells after treatment with CNL (Figure 5C).

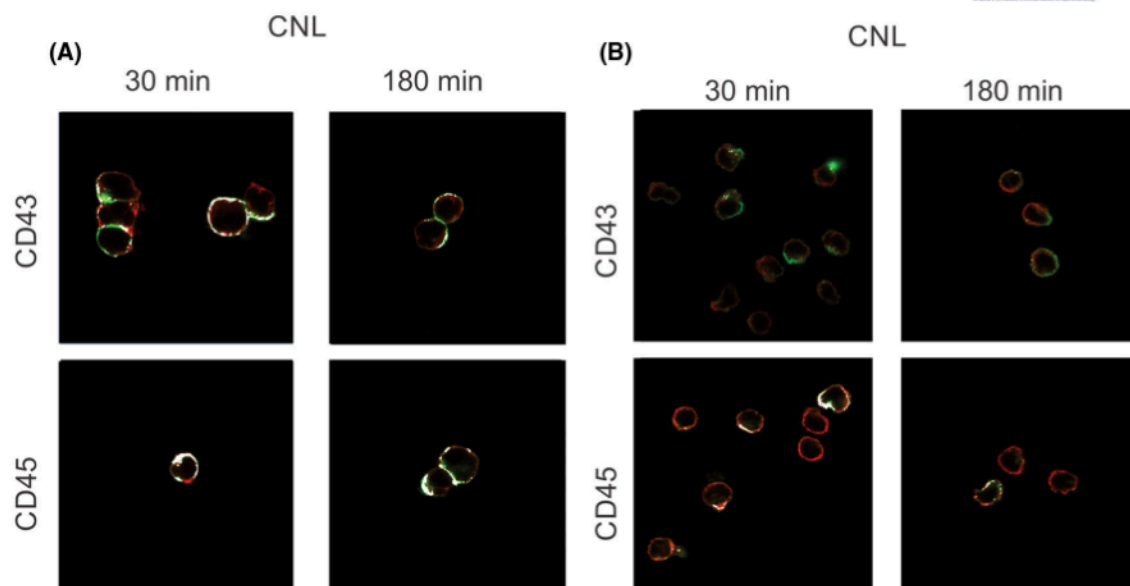


FIGURE 4 Co-localization of *Clitocybe nebularis* lectin (CNL) with its target glycoproteins on Jurkat and Tall-104 cells. Jurkat (A) and Tall-104 (B) cells incubated with CNL for 30 min and 3 h and labeled with antibodies against CNL (green) together with CD45 (red) or CD43 (red). Images were acquired at 63× magnification. Control staining of Jurkat and Tall-104 cells with anti-CNL antibodies in the absence of CNL is shown in Figure S7

Furthermore, since it was shown that pre-incubation with protein kinase inhibitors blocks anti-CD45 antibody-induced cell aggregation³¹ and death,³² we pre-incubated Jurkat cells with dasatinib, a small molecule inhibitor of Abl and Src family tyrosine kinases, including the lymphocyte-specific protein tyrosine kinase p56Lck, and low doses of staurosporine, a nonselective protein kinase C inhibitor before the addition of CNL. However, we failed to detect significant changes in either homotypic aggregation (not shown) or viability of Jurkat cells pre-treated with protein kinase inhibitors after 24 h of incubation with CNL (Figure 5D). Treatment with tunicamycin, a well-known inhibitor of N-glycosylation did not affect CNL-mediated cell aggregation (Figure 5E). Furthermore, since CD45 tyrosine phosphatase activity was shown to be regulated by O-glycosylation and sialylation,³³ we compared the expression of enzymes involved in LacDiNAc synthesis in these cell lines. The enzymes that transfer GalNAc from UDP-GalNAc to the non-reduced terminal N-acetylglucosamine (GlcNAc) of N- and O-glycans in a β -1,4-linkage are β 4-N-acetylgalactosaminyltransferases (β 4GalNAcTs), β 4GalNAcT3 (β 4GalNAcT3, GeneBank AB089940), and β 4GalNAcT4 (β 4GalNAcT4, GeneBank AB089939).¹⁴ They show different tissue distribution in humans, in which the β 4GalNAcT3 gene is expressed abundantly in the stomach, colon, and testis, while the β 4GalNAcT4 gene is expressed in the ovary and brain.^{14,34} Furthermore, β 4GalNAcTs expression has been shown to be closely associated with tumor formation, whereas the expression levels of β 4GalNAcT3, β 4GalNAcT4, and the

LacDiNAc groups are differentially regulated in individual tumors.¹⁴ Our results show different expression levels of these enzymes in different cell lines, with Tall-104 cells showing the highest expression of both enzymes. Compared to Jurkat cells, β 4GalNAcT3 expression was significantly lower in Raji, K562, and HL-60 cells and higher in NK-92 and Tall-104 cells. Compared to Jurkat cells, β 4GalNAcT4 expression was lower only in Raji cells and higher in NK-92 and Tall-104 cells (Figure 5F).

3.6 | WFA is cytotoxic for Jurkat, Tall-104, and Hut-87 cells

The only other well-characterized lectin that specifically binds to the LacDiNAc disaccharide is WFA, which belongs to the leguminous lectin family and shares the Jelly Roll fold with the well-known plant lectin Concanavalin A.^{6,35} Different WFA concentrations (5 μ g/ml for Jurkat (Figure 6A), 25 μ g/ml for Tall-104 (Figure 6F), and 50 μ g/ml for Hut-87 (Figure S5A)) significantly decreased cell viability. Flow cytometry analysis showed a significant increase in Annexin V+ cells after 4 h of incubation with WFA which did not significantly increase at the longer incubation time point (24 h) for all cell lines tested. However, the percentage of PI+, i.e., primary/secondary necrotic, cells was approximately 80% in all cell lines and remained unchanged after 24 h, implying that WFA induces necrotic-like cell death very quickly (Figures 6B,G and S5B). For all cell lines, it was shown that the 4 h

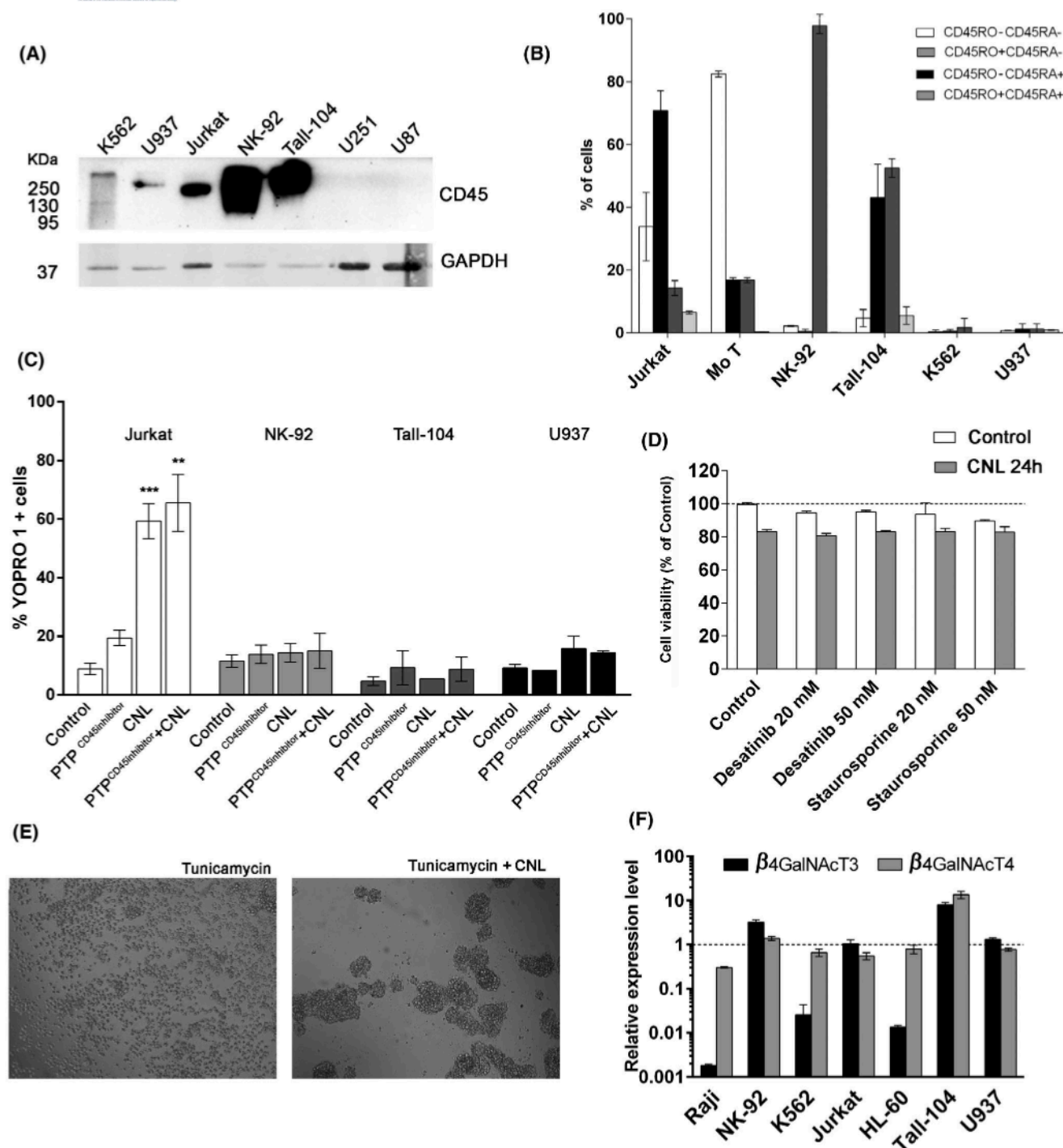


FIGURE 5 The binding of *Clitocybe nebularis* lectin (CNL) to CD45 in different cell lines. (A) Western blot analysis of CD45 expression in different cell lines. (B) Flow cytometry analysis of the expression of two different isoforms of CD45 (CD45RA and CD45RO) in different cell lines. (C) Flow cytometry analysis of the viability of Jurkat, NK-92, Tail-104, and U937 cells after 24 h of incubation with CNL in the presence or absence of a specific inhibitor of CD45-associated protein tyrosine phosphatase (PTP) (10 μM). Asterisks above bars indicate statistically significant differences (** $p < .01$; *** $p < .001$) between the control and CNL-treated cells. (D) The viability of Jurkat cells after 1 h of pretreatment with dasatinib and staurosporine followed by 24 h of incubation with (grey bars) or without (white bars) 50 μg/ml of CNL. (E) Brightfield images of Jurkat cells treated with tunicamycin for 24 h and with (right) or without (left) 50 μg/ml of CNL for an additional 4 h. (F) The relative expression levels of β4GalNAcT3 and β4GalNAcT4 in different cell lines were determined by qPCR. Data from three independent experiments are presented as mean ± standard deviation

incubation with WFA induces homotypic aggregation of cells, which increases after 24 h (Figures 6D,H and S5C). Both homotypic aggregation and the cytotoxic effect of WFA were blocked by pre-incubating cells with 0.1 M lactose (Figure 6D,H). Western blot analysis of Jurkat cell culture medium revealed a significant release of HMGB1 that increased with longer incubation periods (Figure 6C). Strong colocalization of WFA with the CD45 was detected in both Jurkat and Tall-104 cells, whereas co-localization with CD43 was less pronounced (Figure 6E,I).

4 | DISCUSSION

In the past decade, fungal lectins have attracted growing interest due to their antitumor activities. Several lectins isolated from edible mushrooms have shown antiproliferative activity against different human cell lines.^{36–39} However, that antitumor ability stems from the induction of programmed cell death has so far only been demonstrated for the lectins isolated from the *Kurokawa* mushroom⁴⁰ and *Agrocybe aegerita* (AAL).⁴¹ Our testing on multiple tumor cell lines of immune and non-immune origin showed that CNL induces atypical cell death selectively on Jurkat cells. This distinguishes CNL from most of the fungal lectins described thus far that has been shown to be toxic on multiple human cell lines.^{36,42}

Many of the biological activities of lectins are based on multivalent lectin carbohydrate interactions, as shown for human homodimeric galectin-1, which induces apoptosis of human T cells by cross-linking and segregating specific receptors on the cell surface.⁴³ Although CNL possesses only one carbohydrate-binding site per monomer, it is, as a homodimeric structure, bivalent.^{19,20} Dimerization and carbohydrate-binding were shown to be necessary for CNL interaction with Jurkat cells.²⁰ Similar results were obtained for NK-92 and Tall-104 cells (data not shown). Furthermore, the cytotoxic effect on Jurkat cells was not detected upon incubation with either the non-dimerizing CNL mutant or preincubation with lactose.²⁰ Among mushroom lectins, the requirement for dimerization and bivalent carbohydrate-binding for cytotoxicity has so far only been shown for the *A. aegerita* lectin.⁴¹

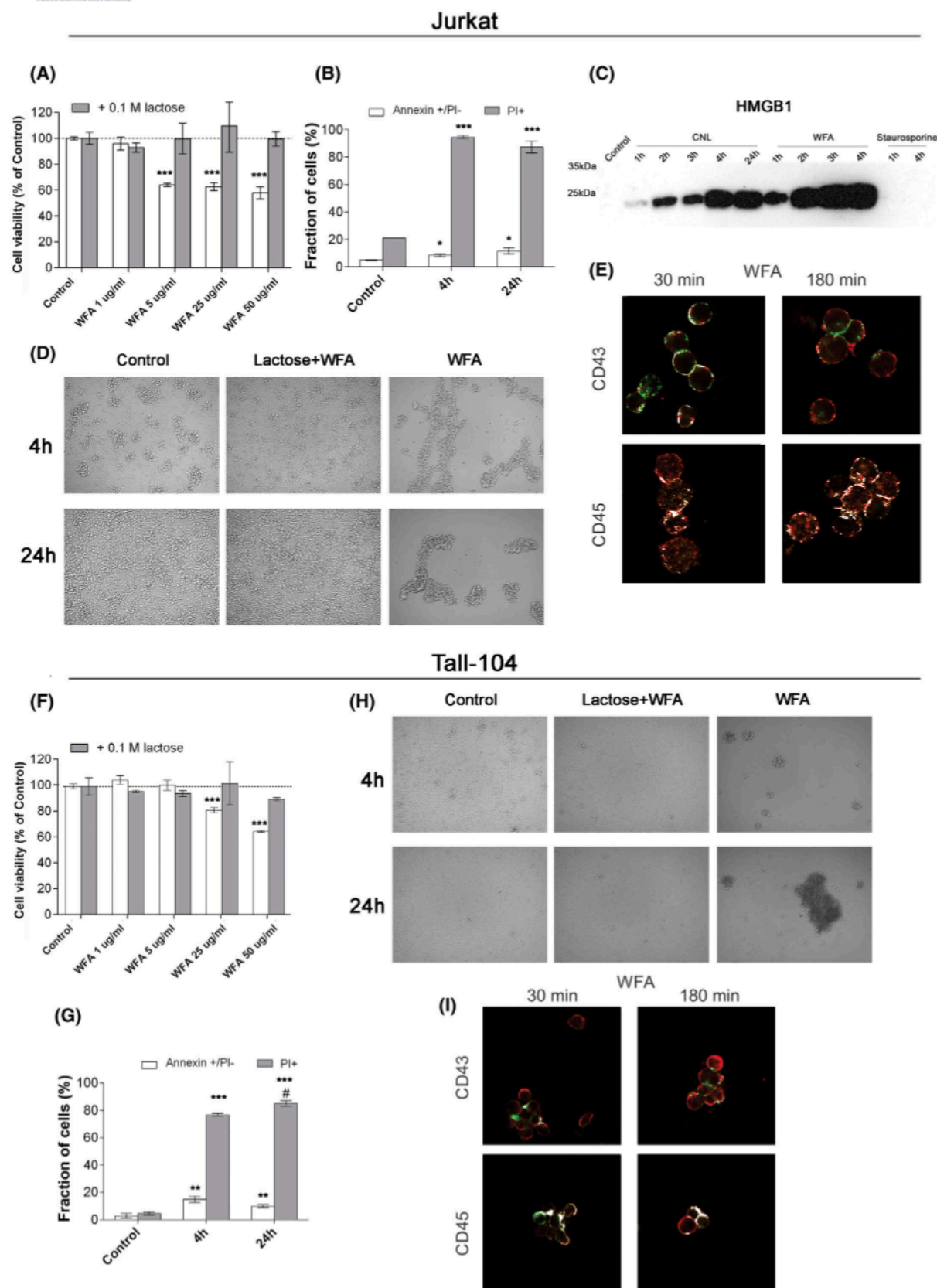
In this study, CNL bound to the cell surface almost immediately and was still detected on the cell surface after 48 h. Unlike galectin-1 and *A. aegerita* lectin, which were shown to exert their cytotoxic function by invading cells upon binding,⁴¹ CNL internalization was not detected even after 18 h of incubation, implying that it recognizes and cross-links specific glycan ligands on Jurkat cells, which leads to signal transduction and subsequent cytotoxic effects. The same functional pathway was shown for three other β -trefoil-type lectins: *Rhizoctonia*

solani agglutinin (RSA), *Sclerotinia sclerotiorum* agglutinin (SSA), and *Coprinopsis cinerea* lectin 2 (CCL2) that induced apoptosis of their respective target cells without cell internalization.¹² However, for another β -trefoil-fold lectin, *Boletus edulis* lectin (BEL) carbohydrate-binding and internalization into cells were shown to be important for its antiproliferative effect.⁴⁴ Interestingly, another representative of the β -trefoil-type lectins, *Macropleiota procera* lectin, was shown to be non-toxic for different human cell lines,⁴⁵ implying different functional pathways among structurally similar β -trefoil-fold lectins.

Similarly, to galectin-1 binding to Jurkat cells, CNL binding stimulates the cell surface expression of phosphatidylserine, an early indicator of apoptosis⁴⁶ reviewed in Ref. [32]. Furthermore, galectin-1-mediated ligation of CD45 was shown to be necessary for this process in Jurkat cells. However, unlike galectin-1-induced cell death,^{32,46} CNL-induced cell death was not inhibited by the pan-caspase inhibitor. In addition, whereas kifunensine (which blocks the formation of complex-type N-glycans) inhibited phosphatidylserine exposure on the cell membrane of Jurkat cells treated with recombinant human galectin-1,⁴⁷ tunicamycin (an inhibitor of the initial step of protein N-glycosylation) did not affect the induction of phosphatidylserine (not shown) nor homotypic aggregation of CNL-treated Jurkat cells. This suggests that these effects are mediated through binding to O-linked glycans.

CNL also causes chromatin condensation and membrane and mitochondrial hallmarks of apoptosis, which occur without the activation of caspase-3.⁴⁶ To better understand the signaling pathways involved in CNL-induced cell death, we attempted to block cell death with inhibitors that have been shown to block lymphocyte apoptosis and different forms of programmed necrosis. The Fas-FasL pathway exhibited no involvement in CNL-induced cell death. Furthermore, the inhibition of RIPK3 and a wide range of lysosomal protease inhibitors that have been shown to block several types of programmed necrosis²³ failed to significantly affect the cytotoxic effects of CNL. We have shown that CNL induces the time-dependent release of HMGB1, which exhibits proangiogenic⁴⁸ as well as chemotactic activity on several types of immune cells, including monocytes, macrophages, neutrophils, dendritic cells,^{49,50} enterocytes, smooth muscle cells, and endothelial cells.^{48,51} Moreover, ferrostatin-1, an inhibitor of ferroptosis, an iron-dependent form of regulated necrosis,⁵² had no effect on CNL cytotoxicity and CNL did not induce alkaliptosis, a pH-dependent form of cell death⁵³ (Figure S6).

Our study to identify CNL-interacting molecules points to the heavily glycosylated external domains of CD43 and CD45 as major CNL targets on the membrane



of Jurkat cells. These are the most abundant glycoproteins on the lymphocyte cell surface that are involved in many cell functions.^{29,54} The binding of CNL to the carbohydrate part of CD43 and CD45 could be inhibited by

lactose, as detected by the lack of signal obtained from the solubilized Jurkat membrane preparations when lactose was added before CNL binding. It is well established that CD45 surface expression alone does not render cells

FIGURE 6 The effects of *Wisteria floribunda* agglutinin (WFA) on Jurkat and Tall-104 cells. The viability of Jurkat (A) and Tall-104 (F) cells after 4 h incubation with different WFA concentrations. Asterisks above bars indicate statistically significant differences ($***p < .001$) between the control and WFA-treated cells. Flow cytometric analysis of Annexin V/PI-stained Jurkat (B) and Tall-104 (G) cells after 4 h and 24 h of incubation with 50 $\mu\text{g}/\text{ml}$ of WFA. Bars represent means \pm SD of the percentage of control cells (white bars). The data were analyzed using one-way analysis of variance (ANOVA) where $*(p < .05)$; $** (p < .01)$; $*** (p < .001)$ indicate significant difference in comparison with the untreated (control) group; $^\# (p < .05)$ indicates significant difference in comparison with the 4 h treated group. (C) Western blot analysis of high-mobility group box 1 (HMGB1) release into the cell culture medium at indicated time points after the addition of *Clitocybe nebularis* lectin (CNL), WFA, and staurosporine. Brightfield images of Jurkat (D) and Tall-104 (H) cells after 4 h and 24 h treatment with 100 $\mu\text{g}/\text{ml}$ of WFA in the presence or absence of 0.1 M lactose. Images were acquired at 10 \times magnification. Jurkat (E) and Tall-104 (I) cells incubated with FITC-conjugated WFA (green) for 30 min and 3 h and labeled with antibodies against CD45 and CD43 and secondary goat anti-rabbit antibodies conjugated with Alexa Fluor 555 (red). Images were acquired at 63 \times magnification

sensitive to CD45-mediated cell death.³² However, the use of mAbs for specific CD45 epitopes provides unequivocal evidence that cross-linking of CD45, alone or with activating signals, can initiate cell death.³² CNL-induced cell death displays several similarities with CD45-ligation-induced cell death. First, it appears to be independent of CD45 phosphatase activity, as the inhibition of phosphatase did not block the cytotoxic effects of CNL. Studies showed that a CD45 mutant molecule lacking the functional phosphatase domain can mediate the effects of mAbs leading to cell death.³² Second, the CNL-induced apoptotic process, although showing hallmarks of apoptosis such as decreased mitochondrial membrane potential and phosphatidylserine translocation, does not result in caspase activation, which is also a prominent feature of CD45-ligation-induced apoptosis.³² Third, CNL-mediated cell death is very rapid, with approximately 60% of cells dying within the first 4 h of the treatment. Similarly, CD45-mediated cell death was shown to be very rapid, displaying maximum effects within 6–8 h. However, contrary to previous studies showing efficient blockade of CD45-mediated cell death with tyrosine kinase inhibitors, such as protein kinase C inhibitor, sphingosine, and herbimycin A,³² we were not able to demonstrate inhibition of CNL-induced cell death using dasatinib and low doses of staurosporine. Therefore, although cell death via CNL displays morphological similarities to apoptosis via CD45, the latter mode of cell death is considered to be a cytoplasmic, non-inflammatory cell death, generating signals sufficient to induce phagocytosis.

CNL-induced cell death is characterized by the condensation of nuclear chromatin, exposure of phosphatidylserine without the activation of caspases, and leakage of the nuclear protein HMGB1 into the cell culture medium—features that collectively suggest an atypical form of cell death. Some examples of the successful killing of neoplastic cells by alternative cell death pathways have already been reported in the literature. For instance, CD47 ligation by thrombospondin or by specific antibodies has been shown to induce caspase-independent cell death in B-cell lymphocytic leukemia cells isolated from patients.³²

Although the expression of different CD45 isoforms changes with the maturation and activation status of T cells, direct cross-linking of specific isoforms is likely not the case, as isoform-specific mAbs are less efficient in inducing apoptosis.⁵⁵ The susceptibility of certain cells to CD45-induced cell death could be, however, increased by the spontaneous homodimerization of CD45 molecules as well as their interaction with cis-interacting partners at the cell surface, such as CD2, CD7, CD26, and CD90, or subcellular localization into specialized lipid microdomains that could allow the transmission of death signals. The extracellular and transmembrane domains of CD45 were shown to mediate lateral associations with other cell-surface proteins such as T-cell receptor CD4, CD2, CD7, CD90, and lymphocyte function-associated antigen (LFA)-1.⁵⁶ Finally, apart from CD45, the effects of CNL on Jurkat cells could be a consequence of its binding to CD43 receptors, as a number of studies have shown that CD43 engagement induces apoptosis of T cells and hematopoietic progenitor cells.^{57–60}

Homotypic aggregation of Jurkat cells was almost instant upon the addition of CNL and increased with longer incubation times. This can be partially attributed to CD45 binding, as CD45 has been shown to regulate adhesion mediated by the binding of integrin LFA-1 to intercellular adhesion molecule (ICAM)-1 and ICAM-3 and to induce homotypic interactions in activated human T cells³² and thymocytes.³³ In addition, CD43 is thought to mediate antiadhesive effects due to the physical barrier formed by its highly negatively charged and rigid rod-like structure. Accordingly, one study has demonstrated that CD43-deficient T cells have increased adhesive properties.⁶¹ Upon the addition of anti-CD43 mAbs, the aggregation process starts within minutes and reaches a maximum level after 6–18 h. Therefore, the aggregation of Jurkat cells upon CNL addition could be a consequence of CD43 cross-linking and masking of an antiadhesive process. In U937 cells, the serine/threonine phosphorylation pathway and activation of protein kinase C act as a negative regulatory mechanism of CD43-induced aggregation, as the nonselective protein kinase C inhibitor staurosporine did

not inhibit but even augmented CD43-induced homotypic aggregation.⁶² In line with this data, dasatinib (a protein tyrosine kinase inhibitor targeting the Src family tyrosine kinases and Abl family kinases) and staurosporine failed to abolish CNL-induced homotypic aggregation of Jurkat cells. It is worth noting that cell glycolipids as potential targets were also studied by lectin blot analysis on thin layer chromatography-resolved glycolipids as described⁶³; however, no apparent targets of CNL binding were observed.

In normal PBMCs, no CNL binding or cytotoxicity was detected. This is similar to the case of the already well-studied *Agaricus bisporus* lectin (ABL), which selectively inhibits the proliferation of human malignant epithelial cell lines without toxicity for normal cells.³⁶ The selectivity of the ABL derives from its binding to the Thomsen-Friedenreich antigen (the T-antigen or disaccharide Gal β 1-3GalNAc), which is bound to either serines or threonines in glycoproteins and exposed on the surface of neoplastic cells.⁶⁴ Similarly, the presence of the disaccharide LacDiNAc motif, upregulated mostly on neoplastic cells, is required for CNL binding.²⁰ The expression of the enzymes that are required for LacdiNAc synthesis was not significantly higher in Jurkat cells compared to other cells used in the study in which CNL showed no toxicity, indicating that glycosylation alone is not the cause of CNL selectivity. The same specificity for LacdiNAc is shared only with WFA.⁶ Both CNL and WFA form hydrogen bonds exclusively with the GalNAc moiety. GalNAc forms six hydrogen bonds with CNL and seven hydrogen bonds with WFA; WFA also forms a larger buried surface area to the GlcNAc moiety than CNL.⁶ Both lectins have been shown to bind to Jurkat cells, induce DNA condensation and phosphatidylserine exposure on cell surfaces, and trigger HMGB1 release. However, we have shown that, in addition to Jurkat cells, WFA is cytotoxic to Tall-104 and Hut-87 cells as well. This difference in selectivity may be attributed to the size, fold, and quaternary structure of the active forms of CNL compared with WFA. The molecular mass of the CNL dimer is 32 kDa, while that of the WFA tetramer is 110 kDa. Another difference is probably in the secondary glycan-binding specificity of these lectins that specifically binds LacdiNAc. However, CNL also shows specificity for GalNAc α 1-3[Fuc α 1-2]Gal β -terminating glycans,^{12,20} while WFA binds to GalNAc- and Gal-terminating glycans.³⁵

In conclusion, our results indicate that CNL binds to several types of leukemia cells but specifically kills only one type of cancer cell line that is representative of acute T cell leukemia (Jurkat cells) through a mechanism distinct from the other forms of programmed cell death reported to date. This selective targeting of Jurkat T cells may reflect the potential applicability of CNL in novel strategies for treating and/or detecting acute T cell leukemia.

ACKNOWLEDGMENTS

We would like to acknowledge Eva Lasič for the critical reading of the manuscript.

DISCLOSURES

The authors declare no conflict of interest. The funders had no role in the design of the study; in the collection, analyses, or interpretation of data; in the writing of the manuscript, or in the decision to publish the results.

AUTHOR CONTRIBUTIONS

Conceptualization: Milica Perišić Nanut, Jerica Sabotič. *Methodology:* Milica Perišić Nanut, Simon Žurga, Špela Konjar, and Mateja Prunk. *Validation:* Jerica Sabotič. *Writing—original draft preparation:* Milica Perišić Nanut. *Writing—review and editing:* Milica Perišić Nanut, Jerica Sabotič, Simon Žurga, Špela Konjar, Mateja Prunk, and Janko Kos. *Funding acquisition:* Janko Kos. All authors have read and agreed to the published version of the manuscript.

DATA AVAILABILITY STATEMENT

The data that support the findings of this study are available on request from the corresponding author. The data are not publicly available due to privacy or ethical restrictions.

ORCID

Milica Perišić Nanut  <https://orcid.org/0000-0003-2314-2733>

Špela Konjar  <https://orcid.org/0000-0002-8969-0233>

Mateja Prunk  <https://orcid.org/0000-0002-9117-633X>

Janko Kos  <https://orcid.org/0000-0002-4228-3518>

Jerica Sabotič  <https://orcid.org/0000-0002-2404-0192>

REFERENCES

1. Muramatsu T. Development. Carbohydrate recognition in spermatogenesis. *Science*. 2002;295:53-54.
2. Pereira MS, Alves I, Vicente M, et al. Glycans as key checkpoints of T cell activity and function. *Front Immunol*. 2018;9:2754.
3. Erbacher A, Gieseke F, Handgretinger R, Muller I. Dendritic cells: functional aspects of glycosylation and lectins. *Hum Immunol*. 2009;70:308-312.
4. Haltiwanger RS, Lowe JB. Role of glycosylation in development. *Annu Rev Biochem*. 2004;73:491-537.
5. Van Dyken SJ, Green RS, Marth JD. Structural and mechanistic features of protein O glycosylation linked to CD8+ T-cell apoptosis. *Mol Cell Biol*. 2007;27:1096-1111.
6. Haji-Ghassemi O, Gilbert M, Spence J, et al. Molecular basis for recognition of the cancer glycomarker, LacdiNAc (GalNAc[β 1 \rightarrow 4]GlcNAc), by *Wisteria floribunda* agglutinin. *J Biol Chem*. 2016;291:24085-24095.
7. Xu Y, Sette A, Sidney J, Gendler SJ, Franco A. Tumor-associated carbohydrate antigens: a possible avenue for cancer prevention. *Immunol Cell Biol*. 2005;83:440-448.

8. Schietinger A, Philip M, Schreiber H. Specificity in cancer immunotherapy. *Semin Immunol*. 2008;20:276-285.
9. Esko JD. Chapter 28. Microbial carbohydrate-binding proteins. In: Varki A, Cummings R, Esko J, Freeze H, Hart G, Marth J, eds. *Essentials of Glycobiology*. Cold Spring Harbor Laboratory Press; 1999:375-386.
10. Mody R, Joshi S, Chaney W. Use of lectins as diagnostic and therapeutic tools for cancer. *J Pharmacol Toxicol Methods*. 1995;33:1-10.
11. Yuan M, Itzkowitz SH, Boland CR, et al. Comparison of T-antigen expression in normal, premalignant, and malignant human colonic tissue using lectin and antibody immunohistochemistry. *Can Res*. 1986;46:4841-4847.
12. Sabotić J, Kos J. CNL-*Clitocybe nebularis* lectin—the fungal GalNAc β 1-4GlcNAc-binding lectin. *Molecules*. 2019;24:4204.
13. Manzella SM, Hooper LV, Baenziger JU. Oligosaccharides containing β 1,4-linked N-acetylgalactosamine, a paradigm for protein-specific glycosylation. *J Biol Chem*. 1996;271:12117-12120.
14. Hirano K, Matsuda A, Shirai T, Furukawa K. Expression of LacdiNAc groups on N-glycans among human tumors is complex. *Biomed Res Int*. 2014;2014:981627.
15. Fukushima K, Satoh T, Baba S, Yamashita K. α 1,2-Fucosylated and β -N-acetylgalactosaminylated prostate-specific antigen as an efficient marker of prostatic cancer. *Glycobiology*. 2009;20:452-460.
16. Machado E, Kandzia S, Carilho R, Altevogt P, Conradt HS, Costa J. N-Glycosylation of total cellular glycoproteins from the human ovarian carcinoma SKOV3 cell line and of recombinantly expressed human erythropoietin. *Glycobiology*. 2011;21:376-386.
17. Peracaula R, Royle L, Tabarés G, et al. Glycosylation of human pancreatic ribonuclease: differences between normal and tumor states. *Glycobiology*. 2003;13:227-244.
18. Che M-I, Huang J, Hung J-S, et al. β 1, 4-N-acetylgalactosaminyltransferase III modulates cancer stemness through EGFR signaling pathway in colon cancer cells. *Oncotarget*. 2014;5:3673-3684.
19. Pohleven J, Obermajer N, Sabotić J, et al. Purification, characterization and cloning of a ricin B-like lectin from mushroom *Clitocybe nebularis* with antiproliferative activity against human leukemic T cells. *Biochem Biophys Acta*. 2009;1790:173-181.
20. Pohleven J, Renko M, Magister Š, et al. Bivalent carbohydrate binding is required for biological activity of *Clitocybe nebularis* lectin (CNL), the N, N'-diacetyllactosediimine (GalNAc β 1-4GlcNAc, LacdiNAc)-specific lectin from basidiomycete *C. nebularis*. *J Biol Chem*. 2012;287:10602-10612.
21. Sawai H, Domae N. Discrimination between primary necrosis and apoptosis by necrostatin-1 in Annexin V-positive/propidium iodide-negative cells. *Biochem Biophys Res Comm*. 2011;411:569-573.
22. Jacobson LS, Lima H Jr, Goldberg MF, et al. Cathepsin-mediated necrosis controls the adaptive immune response by Th2 (T helper type 2)-associated adjuvants. *J Biol Chem*. 2013;288:7481-7491.
23. Brojatsch J, Lima H, Kar AK, et al. A proteolytic cascade controls lysosome rupture and necrotic cell death mediated by lysosome-destabilizing adjuvants. *PLoS One*. 2014;9:e95032.
24. Andersson U, Yang H, Harris H. High-mobility group box 1 protein (HMGB1) operates as an alarmin outside as well as inside cells. *Semin Immunol*. 2018;38:40-48.
25. Kim HJ, Park HJ, Park WS, Bae Y. CD43 cross-linking increases the Fas-induced apoptosis through induction of Fas aggregation in Jurkat T-cells. *Exp Mol Med*. 2006;38:357-363.
26. Pericolini E, Gabrielli E, Bistoni G, et al. Role of CD45 signaling pathway in galactoxylomannan-induced T cell damage. *PLoS One*. 2010;5:e12720.
27. Perron M, Saragovi HU. Inhibition of CD45 phosphatase activity induces cell cycle arrest and apoptosis of CD45⁺ lymphoid tumors ex vivo and in vivo. *Mol Pharmacol*. 2018;93:575-580.
28. Trowbridge IS, Thomas ML. CD45: an emerging role as a protein tyrosine phosphatase required for lymphocyte activation and development. *Annu Rev Immunol*. 1994;12:85-116.
29. Irie-Sasaki J, Sasaki T, Penninger JM. CD45 regulated signaling pathways. *Curr Top Med Chem*. 2003;3:783-796.
30. Dang AM, Phillips JA, Lin T, Raveche ES. Altered CD45 expression in malignant B-1 cells. *Cell Immunol*. 1996;169:196-207.
31. Spertini F, Wang AV, Chatila T, Geha RS. Engagement of the common leukocyte antigen CD45 induces homotypic adhesion of activated human T cells. *J Immunol*. 1994;153:1593-1602.
32. Steff AM, Fortin M, Philippoussis F, et al. A cell death pathway induced by antibody-mediated cross-linking of CD45 on lymphocytes. *Crit Rev Immunol*. 2003;23:421-440.
33. Xu Z, Weiss A. Negative regulation of CD45 by differential homodimerization of the alternatively spliced isoforms. *Nat Immunol*. 2002;3:764-771.
34. Gotoh M, Sato T, Kiyohara K, et al. Molecular cloning and characterization of beta1,4-N-acetylgalactosaminyltransferases IV synthesizing N,N'-diacetyllactosediimine. *FEBS Lett*. 2004;562:134-140.
35. Sato T, Tateno H, Kaji H, et al. Engineering of recombinant *Wisteria floribunda* agglutinin specifically binding to GalNAc β 1,4GlcNAc (LacdiNAc). *Glycobiology*. 2017;27:743-754.
36. Yu L, Fernig DG, Smith JA, Milton JD, Rhodes JM. Reversible inhibition of proliferation of epithelial cell lines by *Agaricus bisporus* (edible mushroom) lectin. *Can Res*. 1993;53:4627.
37. Kawagishi H, Nomura A, Mizuno T, Kimura A, Chiba S. Isolation and characterization of a lectin from *Grifola frondosa* fruiting bodies. *Biochim Biophys Acta*. 1990;1034:247-252.
38. Lin J-Y, Chou T-B. Isolation and characterization of a lectin from edible mushroom, *Volvariella volvacea*. *J Biochem*. 1984;96:35-40.
39. Hassan MA, Rouf R, Tiralongo E, May TW, Tiralongo J. Mushroom lectins: specificity, structure and bioactivity relevant to human disease. *Int J Mol Sci*. 2015;16:7802-7838.
40. Koyama Y, Katsuno Y, Miyoshi N, et al. Apoptosis induction by lectin isolated from the mushroom *Boletopsis leucomelas* in U937 Cells. *Biosci Biotechnol Biochem*. 2002;66:784-789.
41. Yang N, Li D-F, Feng L, et al. Structural basis for the tumor cell apoptosis-inducing activity of an antitumor lectin from the edible mushroom *Agrocybe aegerita*. *J Mol Biol*. 2009;387:694-705.
42. Zhao C, Sun H, Tong X, Qi Y. An antitumor lectin from the edible mushroom *Agrocybe aegerita*. *Biochem J*. 2003;374:321-327.
43. Perillo NL, Pace KE, Seilhamer JJ, Baum LG. Apoptosis of T cells mediated by galectin-1. *Nature*. 1995;378:736-739.
44. Bovi M, Cenci L, Perduca M, et al. BEL β -trefoil: a novel lectin with antineoplastic properties in king bolete (*Boletus edulis*) mushrooms. *Glycobiology*. 2013;23:578-592.

45. Žurga S, Perišić Nanut M, Kos J, Sabotić J. Fungal lectin Mpl enables entry of protein drugs into cancer cells and their sub-cellular targeting. *Oncotarget*. 2017;8:26896-26910.
46. Lesage S, Steff AM, Philippoussis F, et al. CD4⁺ CD8⁺ thymocytes are preferentially induced to die following CD45 cross-linking, through a novel apoptotic pathway. *J Immunol*. 1997;159:4762-4771.
47. Karmakar S, Stowell SR, Cummings RD, McEver RP. Galectin-1 signaling in leukocytes requires expression of complex-type N-glycans. *Glycobiology*. 2008;18:770-778.
48. Mitola S, Belleri M, Urbinati C, et al. Cutting edge: extracellular high mobility group box-1 protein is a proangiogenic cytokine. *J Immunol*. 1990;146:12-15.
49. Dumitriu IE, Baruah P, Manfredi AA, Bianchi ME, Rovere-Querini P. HMGB1: guiding immunity from within. *Trends Immunol*. 2005;26:381-387.
50. Yang D, Chen Q, Yang H, Tracey KJ, Bustin M, Oppenheim JJ. High mobility group box-1 protein induces the migration and activation of human dendritic cells and acts as an alarmin. *J Leukoc Biol*. 2007;81:59-66.
51. Degryse B, Bonaldi T, Scaffidi P, et al. The high mobility group (HMG) boxes of the nuclear protein HMG1 induce chemotaxis and cytoskeleton reorganization in rat smooth muscle cells. *J Cell Biol*. 2001;152:1197-1206.
52. Li J, Cao F, Yin HL, et al. Ferroptosis: past, present and future. *Cell Death Dis*. 2020;11:88.
53. Liu J, Kuang F, Kang R, Tang D. Alkalitosis: a new weapon for cancer therapy. *Cancer Gene Ther*. 2020;27:267-269.
54. Thomas ML. The leukocyte common antigen family. *Annu Rev Immunol*. 1989;7:339-369.
55. Klaus SJ, Sidorenko SP, Clark EA. CD45 ligation induces programmed cell death in T and B lymphocytes. *J Immunol*. 1996;156:2743-2753.
56. Altin JG, Sloan EK. The role of CD45 and CD45-associated molecules in T cell activation. *Immunol Cell Biol*. 1997;75:430-445.
57. Bazil V, Brandt J, Tsukamoto A, Hoffman R. Apoptosis of human hematopoietic progenitor cells induced by crosslinking of surface CD43, the major sialoglycoprotein of leukocytes. *Blood*. 1995;86:502-511.
58. Brown TJ, Shuford WW, Wang WC, et al. Characterization of a CD43/leukosialin-mediated pathway for inducing apoptosis in human T-lymphoblastoid cells. *J Biol Chem*. 1996;271:27686-27695.
59. Cermák L, Šimová S, Pintzas A, Horejsi V, Andera L. Molecular mechanisms involved in CD43-mediated apoptosis of TF-1 cells. Roles of transcription Daxx expression, and adhesion molecules. *J Biol Chem*. 2002;277:7955-7961.
60. Park WS, Chae JS, Jung KC, Choi WJ, Kook MC, Bae Y. Production and the characterization of monoclonal antibody against CD43, K06. *Tissue Antigens*. 2004;63:46-53.
61. Manjunath N, Correa M, Ardman M, Ardman B. Negative regulation of T-cell adhesion and activation by CD43. *Nature*. 1995;377:535-538.
62. Cho JY, Chain BM, Vives J, Horejsi V, Katz DR. Regulation of CD43-induced U937 homotypic aggregation. *Exp Cell Res*. 2003;290:155-167.
63. Barrows BD, Griffiths JS, Aroian RV. *Caenorhabditis elegans* carbohydrates in bacterial toxin resistance. *Methods Enzymol*. 2006;417:340-358.
64. Yu LG. The oncofetal Thomsen-Friedenreich carbohydrate antigen in cancer progression. *Glycoconj J*. 2007;24:411-420.
65. Idziorek T, Estaquier J, De Bels F, Ameisen JC. YOPRO-1 permits cytofluorometric analysis of programmed cell death (apoptosis) without interfering with cell viability. *J Immunol Methods*. 1995;185:249-258.
66. Wessel D, Flügge UI. A method for the quantitative recovery of protein in dilute solution in the presence of detergents and lipids. *Anal Biochem*. 1984;138:141-143.
67. Huang J, Liang J-T, Huang H-C, et al. β 1,4-N-Acetylgalactosaminyltransferase III enhances malignant phenotypes of colon cancer cells. *Mol Cancer Res*. 2007;5:543-552.
68. Liu Y, Liu H, Yang L, et al. Loss of N-Acetylgalactosaminyltransferase-4 orchestrates oncogenic MicroRNA-9 in hepatocellular carcinoma. *J Biol Chem*. 2017;292:3186-3200.
69. Hellemans J, Mortier G, De Paepe A, Speleman F, Vandesompele J. qBase relative quantification framework and software for management and automated analysis of real-time quantitative PCR data. *Genome Biol*. 2007;8:R19.

SUPPORTING INFORMATION

Additional supporting information may be found in the online version of the article at the publisher's website.

How to cite this article: Perišić Nanut M, Žurga S, Konjar Š, Prunk M, Kos J, Sabotić J. The fungal *Clitocybe nebularis* lectin binds distinct cell surface glycoprotein receptors to induce cell death selectively in Jurkat cells. *FASEB J*. 2022;36:e22215. doi:[10.1096/fj.202101056RR](https://doi.org/10.1096/fj.202101056RR)